fibers

MDPI

Review

A Review on Drilling of Multilayer Fiber-Reinforced Polymer Composites and Aluminum Stacks: Optimization of Strategies for Improving the Drilling Performance of Aerospace Assemblies

Gérald Franz [1,*], Pascal Vantomme [1] and Muhammad Hafiz Hassan [2]

[1] Laboratoire des Technologies Innovantes, UR UPJV 3899, Avenue des Facultés, Le Bailly, 80025 Amiens, France
[2] School of Mechanical Engineering, Universiti Sains Malaysia, Nibong Tebal 14300, Malaysia
* Correspondence: gerald.franz@u-picardie.fr

Abstract: In recent years, the use of hybrid composite stacks, particularly CFRP/Al assemblies, and fiber metal laminates (FMLs) has progressively become a convincing alternative to fiber-reinforced polymers (FRPs) and conventional metal alloys to meet the requirements of structural weight reduction in the modern aerospace industry. These new structural materials, which combine greater mechanical properties with low specific mass, are commonly assembled by riveted and bolted joints. The drilling operation, which represents the essential hole-making process used in the aerospace industry, proves particularly challenging when it comes to achieving damage-free holes with tight tolerances for CFRP/Al stacks in one-shot operations under dry conditions due to the dissimilar mechanical and thermal behavior of each constituent. Rapid and severe tool wear, heat damage, oversized drilled holes and the formation of metal burrs are among the major issues induced by the drilling of multi-material stacks. This paper provides an in-depth review of recent advancements concerning the selection of optimized strategies for high-performance drilling of multi-material stacks by focusing on the significant conclusions of experimental investigations of the effects of drilling parameters and cutting tool characteristics on the drilling performance of aerospace assemblies with CFRP/Al stacks and FML materials. The feasibility of alternative drilling processes for improving the hole quality of hybrid composite stacks is also discussed.

Keywords: drilling; CFRP/aluminum stacks; FML; delamination; thrust force; geometrical accuracy; surface roughness; chips; burr

Citation: Franz, G.; Vantomme, P.; Hassan, M.H. A Review on Drilling of Multilayer Fiber-Reinforced Polymer Composites and Aluminum Stacks: Optimization of Strategies for Improving the Drilling Performance of Aerospace Assemblies. *Fibers* **2022**, *10*, 78. https://doi.org/10.3390/fib10090078

Academic Editor: Lucian Blaga

Received: 30 July 2022
Accepted: 5 September 2022
Published: 9 September 2022

1. Introduction

Nowadays, structural weight reduction remains one of the main solutions for improving aircraft performance and promoting energy saving, so much so that over the past few decades, the requirement for lightweight structural materials with high-performance mechanical properties has seen a sharp increase in the modern aerospace industry [1]. Therefore, alternative materials to fiber-reinforced polymers (FRPs) and conventional metal alloys have progressively emerged, and the use of hybrid composite stacks and fiber metal laminates (FMLs) has gained popularity in the aerospace and aeronautics industries. In particular, in highly loaded sections of the fuselage and wings, the use of two- or three-layer metal–composite stack arrangements is fundamental to providing the structural integrity required for service without overly impacting the overall weight [2].

Hybrid composite stacks are composed of multilayer FRPs and metal alloys, such as titanium alloys or aluminum alloys, which allows them to benefit from enhanced properties resulting from the advantages of each stacked material while avoiding their individual weaknesses [3,4]. FRPs are heterogeneous materials that combine lightweight, stiff but

brittle reinforcing fibers (aramid, carbon or glass) bound together by a polymer matrix (thermoplastic or thermoset). The reinforcing phase contributes to improving the mechanical properties of the laminated composite, while the matrix phase transfers the load to inner fibers, protects them from external damage and provides the composite material with its high fracture toughness [5]. For example, several types of FRPs are used in the manufacturing of Airbus A320/A319 components, including aramid fiber-reinforced polymers (AFRPs), which are used in the radome and belly fairing skins, carbon fiber-reinforced polymers (CFRPs), which are incorporated into aircraft wing boxes, horizontal/vertical stabilizers and wing panels, and glass fiber-reinforced polymers (GFRPs), which are found in the fairings, storage room doors, landing gear doors and passenger compartments [6]. Providing the strongest combination of physical and metallurgical properties, including an excellent strength-to-weight ratio, great fracture and fatigue resistance, superior damage threshold energy and exceptional corrosion/erosion resistance, CFRP/Al stacks and their variations have been recognized as one of the most widespread combinations among existing hybrid composite stack configurations [4,7,8]. Furthermore, FML composites, of which the most well-known grades are CARALL®, GLARE® and ARALL®, have carbon, glass, and aramid fibers, respectively, incorporated into epoxy resin and are integrated with aluminum alloy sheets [9,10]. Their growing appeal can be explained by the gain in the tolerance to fatigue crack growth and impact damage, as well as their being between 20 and 25% lighter than aluminum alloys [11].

In aircraft assembly, hybrid composite stacks are essentially fastened by rivets and bolts, which requires producing a large number of holes through entire stacks in a single-shot operation (without prior drilling, deburring or reaming) to minimize positional errors, favor stringent tolerances and reduce production costs [3,12]. Since millions of holes can be required in a commercial aircraft structure, drilling processes are used extensively throughout the aerospace industry [11,13]. Furthermore, for both environmental and economic reasons, dry processes are preferred in aeronautical structures, as drilling without lubricant or coolant significantly reduces the associated costs and improves productivity since post-processing cleaning is no longer required [14,15]. In addition, dry drilling may be considered an environmentally friendly machining process since no chemical additives are needed [16,17].

Joining and fastening efficiency and quality require drilling damage-free holes with tight tolerances, and thus, the quality of drilled holes is critical [18]. In this context, the single-shot drilling of hybrid composite stacks, particularly CFRP/Al, is still challenging because composite laminates and metal alloys exhibit different mechanical and thermal properties and require different machining parameters and tool characteristics specific to each stacked material [3]. Thus, it is well-known that a high cutting speed and low feed rate are recommended when drilling CFRPs [19], while a low cutting speed and high feed rate are advised to achieve better hole quality when drilling Al alloys [7].

Over the last two decades, numerous review articles related to the machining of composite laminates, including CFRP and GFRP materials [1,5,13,18,20–37], metal matrix composites (MMC) [21] and, more recently, nanoparticle (CNF/CNT)-reinforced composite laminates [28] have appeared in the scientific literature. In most cases, these reviews give a comprehensive understanding of the role of drilling parameters, such as spindle speed and feed rate, and drill bits (tool types, geometrical characteristics, tool materials and coatings) on hole surface roughness, thrust force, mechanical and thermal damage of composite materials, delamination and tool wear [1,13,18,20,24,28,29,32,34]. A review of analytical modeling of drilling, restricted to empirical models to calculate a thrust force threshold, called critical thrust force, below which no delamination occurs, was first provided by Khashaba [1] and further extended to artificial and flexible neural network models, abbreviated ANN and FNN, respectively, by Singh et al. [5]. Moreover, many authors have also provided critical reviews on the modeling of conventional machining of composites, including orthogonal cutting and drilling, using molecular dynamics (MD) and 2D or 3D finite element (FE) approaches and their combined use (FE-MD) [21,26,30,33,35,37].

However, few review studies deal with the machining of hybrid composite stacks [3,7,38], and none specifically addresses the drilling of multilayer fiber-reinforced polymer composites and aluminum stacks. Therefore, the primary motivation of this article is to provide a comprehensive review of the drilling of multi-material stacks by focusing on the main issues that occur during the drilling process of CFRP/Al stacks and FML composites. First, key aspects for evaluating the drilling performance of aerospace assemblies are discussed in terms of delamination, hole surface roughness, dimensional accuracy, burr formation, drilling forces, thermal aspects, tool wear and chip formation. Next, the main conclusions of experimental investigations carried out by both industrial and academic communities over the past decades on the effects of drilling parameters and drill bit characteristics on hole quality are summarized. Alternative drilling processes for improving the hole quality of hybrid composite stacks are also addressed. In conclusion, this article aims to provide the keys to understanding the drilling of CFRP/Al stacks and FML composites by highlighting significant results in the scientific literature in order to inform researchers and manufacturers about recent advances concerning the selection of optimized strategies for high-performance drilling of multi-material stacks.

2. Drilling Performance of Aerospace Assemblies

As previously mentioned, drilling represents an essential machining process for joining multilayer FRP composites and aluminum alloys. Despite the fact that the drill successively penetrates through laminated composites and metal parts, it would be incorrect to assume that drilling hybrid composite stacks is identical to drilling these materials separately since the drilled-hole quality of the upper layer is diminished by the evacuation of chips from the lower layer material. The main issues induced by drilling these dissimilar materials are usually rapid and severe tool wear, heat-induced damage, oversized drilled holes, roundness deviation and metal burr formation [3,39,40]. The drilled-hole quality in the aircraft industry can be evaluated from offline parameters, such as delamination, hole wall surface roughness, hole circularity error, hole size deviation and burr height. For example, deteriorated hole surface roughness may contribute to the expansion of areas of concentrated stress [41], thus promoting the probability of fatigue cracks and leading to a reduction in the fatigue life of aircraft structures [42]. Furthermore, the investigation of tool wear or chip formation and the monitoring of online parameters, including drilling forces and drilling temperatures, represent important supplementary outputs required to help in achieving the best drilling performance of aerospace assemblies and reducing drilling-induced delamination [28]. This section provides a description of the aforementioned offline and online parameters and the associated monitoring and assessment methodologies in the drilling process of CFRP/Al stacks and FML composites.

2.1. Delamination in FRPs

Delamination is defined as an inter-ply failure that occurs during the drilling of composite laminates [18]. It is generally accepted as the dominant failure mechanism during the drilling of composite materials. Furthermore, it represents a major issue since it drastically reduces the fatigue strength of the material, which potentially deteriorates the long-term performance of FRPs [43]. This drilling-induced damage is manifested by the splitting between two adjacent layers when the thrust force exceeds the interlaminar bond strength of the material [43]. This phenomenon can be observed both at the machined-hole entry (peel-up delamination) and exit (push-out delamination), as illustrated in Figure 1. When the drill penetrates the top surface of the laminate, the contact between the composite material and the cutting edges of the drill generates a peeling force acting in the axial direction through the slope of the drill flutes, which results in the plies separating from each other and developing a peel-up delamination zone around the drilled-hole entry circumference. The aforementioned peeling force can vary with the tool geometry and friction between the drill and workpiece material [44]. When the drill reaches the exit side of the drilled composite, the uncut thickness thins out, and the uncut plies beneath the

cutting tool then tend to deform, thus giving rise to push-out delamination. In practice, it has been found that push-out delamination is more severe than peel-up delamination due to the greater thrust force exerted by the drill, together with the reduction in the strength of inter-ply bonding [45,46]. In the case of drilling hybrid composite stacks, the mechanism of delamination remains the same as the drilling of single FRPs; only the severity of delamination will be affected by the choice of the stacked sequence. When drilling starts from a laminated composite part to a metal part, push-out delamination is reduced compared with the metal/FRP drilling sequence because the bottom-supporting metal part acts as a backup plate and prevents the deformation of the upper composite part [8,47]. Moreover, in this configuration, peel-up delamination is accentuated by metal chip evacuation [48,49].

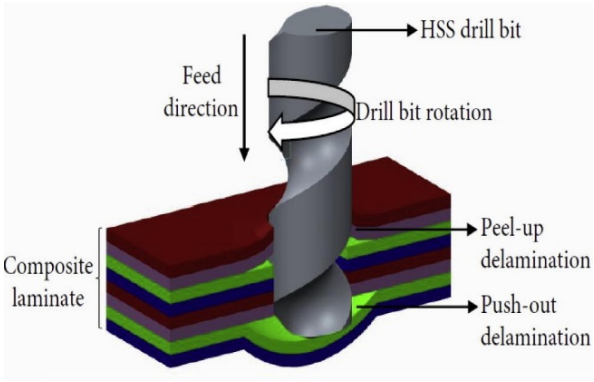

Figure 1. Mechanism of delamination in composite laminate drilling [50].

Many non-destructive measurement technologies, which generally combine image acquisition devices with image processing software, have been developed to monitor the dimensional characteristics, such as size, shape and location, of delamination. These dimensional characteristics are required to quantify drilling-induced delamination. As summarized in several review articles [3,11,13,18,31], the non-destructive methodologies adopted by many researchers to measure delamination are optical microscopy [51–59], digital scanning [55,60–65], ultrasonic C-scan [58,66–71] and X-ray [58,64,67,68,72,73].

Over the past few decades, several methodologies have been provided to assess the level of drilling-induced delamination, and exhaustive reviews of these models can be found in the scientific literature [3,11,13,18,31]. All of these models are based on the determination of a delamination parameter, called the delamination factor, which can be defined in one dimension (1D) [53,57,60,66,72,74], two dimensions (2D) [62,75] or three dimensions (3D) [71] or in an adjusted form [61,76], which combines 1D and 2D delamination factors. Chen [72] was the first to suggest a delamination parameter using the one-dimensional characteristic, i.e., diameter, measured on the drilled hole. This 1D delamination factor, denoted by F_d, is defined as the ratio of the maximum diameter (D_{max}) of the observed delamination zone to the nominal diameter of the drilled hole (D_{nom}). In order to take into account the irregularity of the delamination patterns—in particular, as observed in CFRP drilling—Faraz et al. [62] proposed a 2D delamination factor, denoted by F_a, based on the calculation of the ratio of the area (A_{nom}) related to the maximum diameter (D_{max}) of the delamination zone to the nominal area of the drilled hole (A_{nom}). However, this indicator disregards the contribution of crack length to drilling-induced delamination, since only the area of the delamination zone is taken into account. Both diameters (D_{nom} and D_{max}) and areas (A_{nom} and A_{max}) are shown in Figure 2. The contributions of both crack size and damaged areas are included in the adjusted delamination factor F_{ad}, proposed by Davim et al. [61] and defined as the pondered sum of the 1D delamination factor F_d and the 2D delamination factor F_a. More recently, Xu et al. [71] introduced a 3D delamination factor to incorporate the effect of the interlaminar failure observed inside the FRP. This factor was determined by the arithmetic mean of the 2D delamination factor F_a for each delaminated

layer. Although all of these more advanced delamination factors can accurately assess the real extent of delamination damage, F_d remains the most popular delamination factor used to quantify the level of drilling-induced delamination, as it is easier to use.

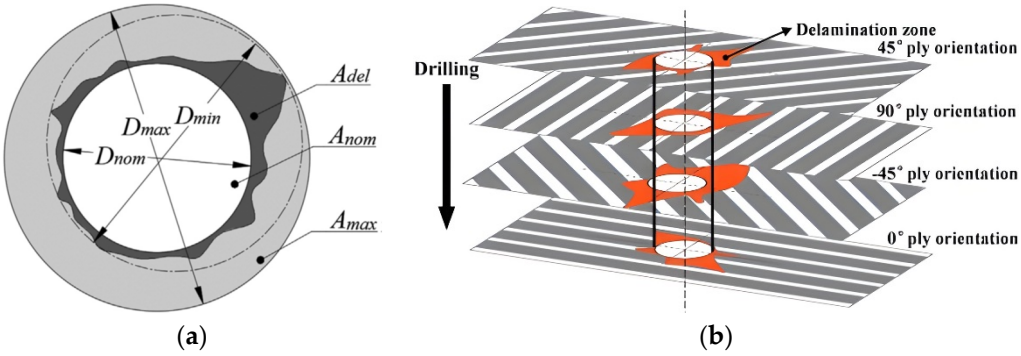

Figure 2. Drilling-induced hole damage of CFRP: (**a**) dimensional characteristics (diameters and areas) used to determine 1D and 2D delamination factors; (**b**) interlaminar delamination [71].

2.2. Surface Roughness in FRPs and Aluminum

It is widely accepted that hole surface roughness is one of the main outputs used to evaluate the drilling performance of composites [13,20,29,77]. This characteristic is measured by monitoring the irregularities of the workpiece surface. Drilling parameters and drill bit geometry greatly impact hole surface roughness [78,79]. The absence of any surface defects (epoxy burn, delamination and void) in the wall of the drilled hole guarantees the high quality of hole surface roughness achieved after the drilling of composite panels. During the drilling process, the cutting parameters and cutting tool properties highly impact the drilled-hole surface roughness. Checking the surface integrity of drilled holes is imperative since irregularities on the surface directly affect the performance of the assembly of aerospace components and may result in major issues, such as excessive wear, fatigue and a drop in the corrosion resistance of the material [80]. Based on previous research [81–84], it is clearly challenging to minimize the hole surface roughness of the composite part, as it has different properties from the metal part. In the case of drilling hybrid composite stacks with an FRP/metal sequence, the metal chip arises by scraping on the hole wall of the composite layer, damaging it further, which means that the hole surface roughness deteriorates much more than in the drilling of the single FRP laminate.

Several roughness parameters, which can be calculated on a line or an area, such as peak-to-valley roughness R_t or S_t, root-mean-square roughness R_q or S_q and ten-point average roughness R_z or S_z, can be used to quantify the amount of roughness, but arithmetic average surface roughness R_a remains commonly used by industries to characterize the machined surface of both metal and composite panels, although it has been established that this parameter is better for measuring the surface roughness of metals than that of composites [85]. Indeed, CFRP surface roughness should be cautiously construed due to the lower measurement reliability in composites compared to that acquired in metals [86]. Arithmetic average surface roughness R_a corresponds to the average absolute height of ordinates of the surface measured from the mean profile height within the sampling length. Nowadays, the maximum acceptable value of R_a for aeronautical structures is 1.6 µm in aluminum panels and 3.2 µm in CFRP panels [49,87,88].

Various surface roughness estimation techniques, which can be distinguished as contact and non-contact methods, are available to estimate the surface roughness of drilled holes [89]. Surface roughness measurements with contact-type methods are performed using a mechanical stylus in direct contact with the tested surface, and laser light is used instead of the stylus when non-contact methods are preferred to assess the surface roughness value. The value of the surface roughness of CFRP drilled holes depends mainly on the stylus path relative to the fiber direction since the main direction of fibers may change from layer to layer; thus, it should be measured several times and averaged [90]. In

the scientific literature, many researchers have studied the drilled-hole surface roughness for CFRP/aluminum stacks [2,7,12,49,77,83,88,90–98] or FML composites [99–102] using a surface profilometer, also called a contact rugosimeter or surface roughness tester, with a sampling length (cutoff) of 0.8 mm. To our knowledge, only Kuo et al. [103] performed the surface roughness measurement of CFRP and aluminum layers using a laser interferometer with a vertical resolution of 0.4–0.6 mm and lateral resolution of 0.1 nm.

2.3. Hole Size and Geometrical Accuracy in FRPs and Aluminum

Dimensional issues are commonly observed when drilling aerospace stacks. Varying dimensional tolerances along the drilled hole may be observed due to the different thermal and mechanical behaviors between composite materials and metal alloys during the drilling process. Moreover, as observed in many studies [12,87,91,104–107], the CFRP drilled-hole diameter remains larger than that measured in the metal part, which can be explained by the detrimental abrasion of the CFRP hole wall resulting from prejudicial metal chip evacuation during the drilling of multi-material stacks. According to Hassan et al. [95], a large difference in diameter between stacked materials would interrupt the assembly process and increase the rate of panels scrapped due to non-compliance with customer specifications.

The accuracy of a drilled hole is commonly assessed using hole size and circularity errors, which are two prominent indicators for evaluating the drilling performance of aerospace assemblies. The deviation of the drilled-hole diameter from the expected hole diameter, known as the nominal hole diameter, is referred to as hole size error. The hole is oversized when the hole size error is positive, while it is qualified as undersized for a negative hole size error. H9 diameter tolerance (+36 µm for a diameter range from 6 to 10 mm) is generally recommended for aeronautical structures since the rivet joint performance is directly related to the amount of hole size error. Moreover, oversized or undersized holes could require additional post-machining operations, which have a direct impact on manufacturing costs [108]. Circularity is a geometrical tolerance that provides information on hole shape and permits the evaluation of the deviation of the circular cross-section of a drilled hole from a perfect circle. It is quantified by the calculation of circularity error, also known as roundness error, which is defined as the radial difference between the maximum inscribing circle and minimum circumscribing circle, as shown in Figure 3. As explained by Ekici et al. [105], the waviness of the hole surface is experimentally determined by taking the difference between the largest and smallest radius values measured by touching the surface of the hole diameter at several points at equal angles.

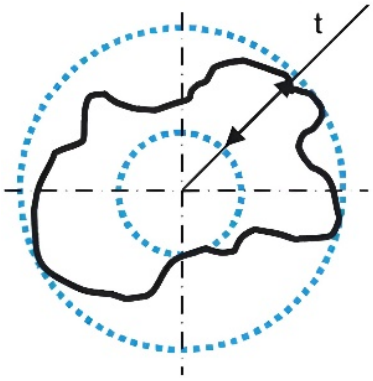

Figure 3. Definition of roundness error.

In practice, hole size and circularity errors are performed on a three-dimensional coordinate measuring machine (CMM) [7,88,93,95,96,103,105,106,109,110].

2.4. Burr Height in Aluminum

A burr is a geometrical defect inherent to metal drilling and can be observed as a raised part present at the periphery of the drilled hole, especially in aluminum alloys, both at the

entry and exit. The occurrence of burrs, which are generally larger at the exit of the hole than at the entry, can be attributed to the plastic deformation of the uncut material during the drilling process. Moreover, burr formation is the result of a combination of larger forces and less resistance in the workpiece material with plastic deformation fracture [111]. Both high localized temperature and thrust force are directly involved in this plastic deformation [91]. As depicted in Figure 4, two types of burrs, namely, uniform and crown, can be identified at the exit of a drilled aluminum plate, depending on workpiece material properties, drilling parameters and cutting forces [109,112]. As explained by Costa et al. [113], entrance hole burrs are formed by the plastic flow of the material, while exit hole burrs are caused by the conformation of the material induced by high compression rates in the center of the hole. The mechanism of exit burr formation in the drilling process is illustrated in Figure 5. Uniform burrs are first initiated at the hole center, where high rates of compression stress are exerted on the material by the chisel edge of the cutting tool, which results in the first fracture. Then, the advancement of the drill bit leads to a second break occurring at the hole periphery when the plastic deformation spreads out from the hole center to the tool edges. Uniform burrs are characterized by small size and uniform height, while crown burrs are large-sized around the exit hole and irregular in shape. In the case of multi-material stacks, burr formation in the metal part represents another issue affecting the drilled-hole quality, which consequently degrades the assembly tolerance and increases component rejection [3]. Furthermore, deburring operations can also account for a considerable amount of the total production cost, up to 30% [114,115]. Therefore, a reduction in the burr height and width induced by the drilling process is required in order to obtain better hole quality, reduce difficulties during fastener positioning and riveting, and lower manufacturing costs.

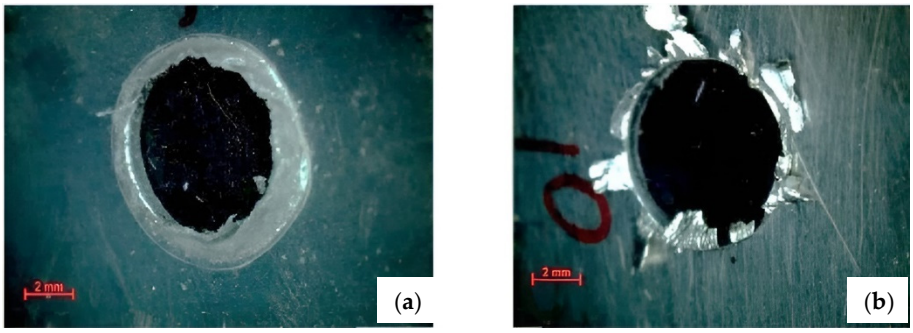

Figure 4. Burr types: (**a**) uniform and (**b**) crown [112].

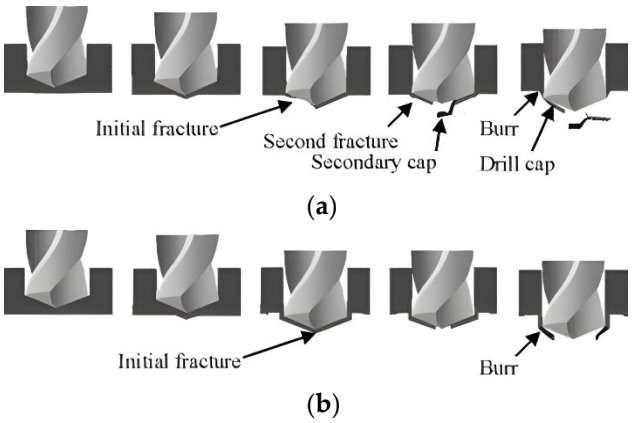

Figure 5. Mechanism of burr formation in drilling process: (**a**) uniform burr and (**b**) crown burr [116].

In the scientific literature, the assessment of the metal burr height resulting from the drilling of multilayer fiber-reinforced polymer composites and aluminum stacks is essentially performed out-of-process using various optical systems, such as a micro-

scope [95,109,112,117,118] or interferometer [88]. Some authors [119,120] have also suggested using in-process evaluation using acoustic emission measurement technology to monitor burr formation.

2.5. Drilling Forces

Drilling forces are among the most outstanding indicators for investigating the machinability of laminated composites and hybrid composite stacks since the quality of the drilled holes, particularly the occurrence of delamination, is directly affected by these parameters [3,45]. Moreover, they offer benefits that can be monitored instantaneously and continuously during the drilling process and thus control the cutting tool life online and help reduce drilling-induced delamination in order to improve the drilling performance of aerospace assemblies. The cutting forces induced by the drilling process are commonly divided into two main components, i.e., thrust force and torque. Thrust force, denoted by F_z, corresponds to the resulting force acting perpendicularly to the workpiece surface, i.e., in the feed direction of the drill bit, required to maintain the cutting tool in the workpiece during its movement in the feed direction. It reflects the tribological behavior of the tool–chip interaction [3]. As suggested by López de Lacalle et al. [121], F_z can be seen as the consequence of the effects of both the indentation of the chisel edge with the material and the cut of the main edges. Therefore, it is possible to decompose F_z into two components, as illustrated in Figure 6. Torque, denoted by M_z, reflects the level of force required to rotate the drill bit during the drilling process. It reflects the tribological behavior of the tool–drilled surface interaction [3]. The forces generated in the other axes' directions are negligible since they are much lower compared to F_z and M_z.

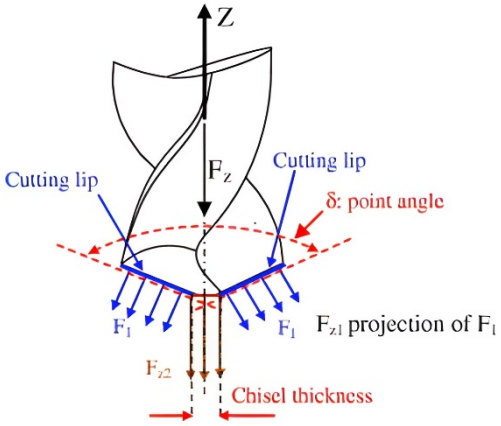

Figure 6. Decomposition of thrust force [122].

Figure 7 shows the typical drilling force signal, plotted as a function of cutting time, observed by Pardo et al. [123] during a single-shot drilling operation of a CFRP/Al stack. In this study, a 10.5 mm thick CFRP comprising 40 unidirectional carbon cured plies enclosed within two M21/1080 glass cured plies was stacked with 10 mm thick aluminum A7010-T651 and drilled with an uncoated tungsten carbide twist drill in dry conditions. Previous studies on single-shot dry drilling of CFRP/Al stacks [7,83,88,93,124,125] with other CFRP and aluminum layer characteristics exhibited the same specific thrust force profile, with values recorded during the drilling of the composite material ranging from two to three times lower than those recorded during the drilling of aluminum alloys. Three main regions, corresponding to the multilayer composite, interface and aluminum alloy drilling zones, are commonly identified in the drilling force signature. In detail, up to seven successive intermediate zones can also be defined. At the beginning of the drilling operation, bringing the tool tip into contact with the top CFRP layer causes an increase in both thrust force and torque components, which are gradually accentuated until the full engagement of the cutting edges with the composite material. As long as the cutting tool is fully engaged through the CFRP part, the amount of cutting forces achieved remains

relatively constant. As proposed by Bonnet et al. [126], the oscillations observed during this period in the drilling force signal, which are more significant for thrust force than torque, can be explained by the alternating fiber orientation. When the chisel edges leave the multilayer composite sheet and begin to penetrate the aluminum plate underneath, a sudden jump in both thrust force and, to a lesser extent, torque is observed. The cutting lips of the drill bit then gradually cut into the aluminum part, and the thrust force thus increases continuously with the advancement of the drilling tool until its maximum value is reached at the end of this drilling region. In addition, it can be noted that both thrust force and torque components are found to be significantly higher when drilling the aluminum layer than the CFRP layer due to differences in properties between these two materials. As previously observed in the CFRP drilling zone, the drilling force signal also fluctuates, which can be explained by the variable chip separation mode at the CFRP/Al interface and by the occurrence of chip clogging, which becomes more likely as the tool penetrates deeper into the multi-material stack [123]. Finally, the emergence of chisel edges from the aluminum layer results in a sharp drop in the cutting forces to zero, when the cutting part of the drill bit completely exits the lower part of the hybrid composite stack.

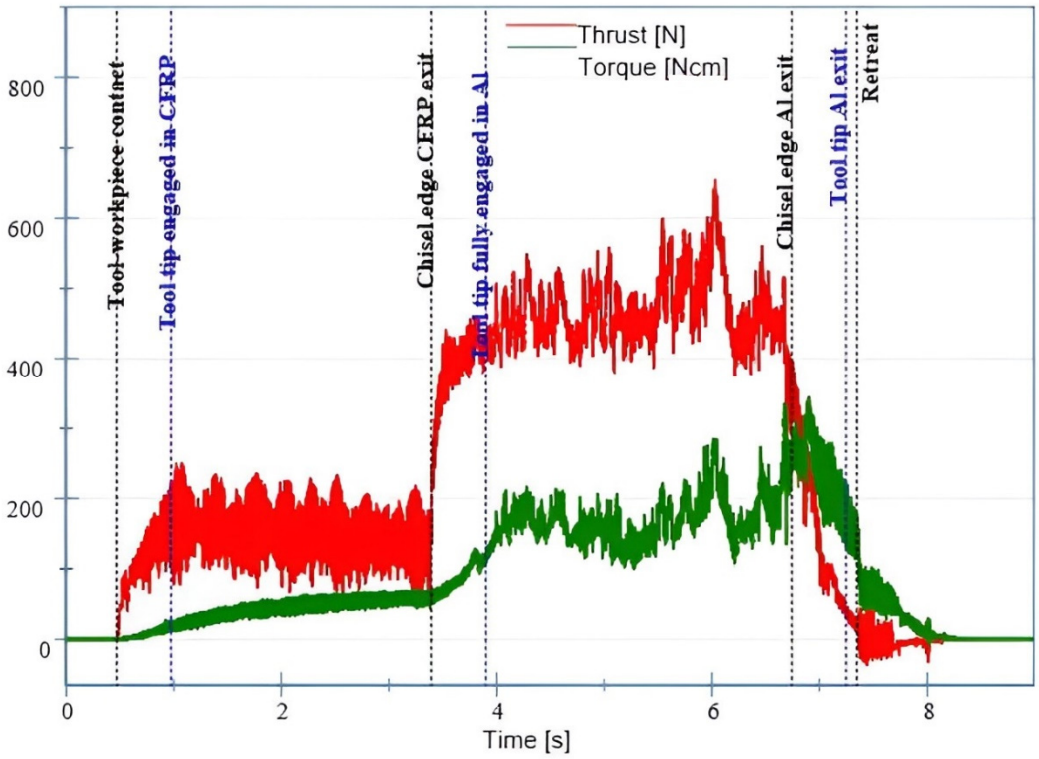

Figure 7. Thrust force evolution as a function of cutting time during the drilling of a CFRP/Al stack [123].

In addition, several recent studies on the drilling of co-cured materials [106,110,127] and FML composites [78,128,129] exhibit a similar thrust force profile to the one observed during the drilling of CFRP/Al stacks, as depicted in Figure 8. As explained previously, thrust force evolution can be related to the variation in the tool–work interaction process, with the same underlying mechanisms. The thrust force achieved when drilling CFRP panels (up and down) is lower than the thrust force generated while drilling the aluminum layer. Furthermore, the drilling of the lower CFRP plate results in a higher thrust force compared to the magnitude of the thrust force observed during the drilling of the upper CFRP plate. This can be attributed to the accumulation and entanglement of aluminum chips around the drill bit as the tool advances through the layers, resulting in more rubbing of the drill against the material during the drilling of the lower CFRP layer.

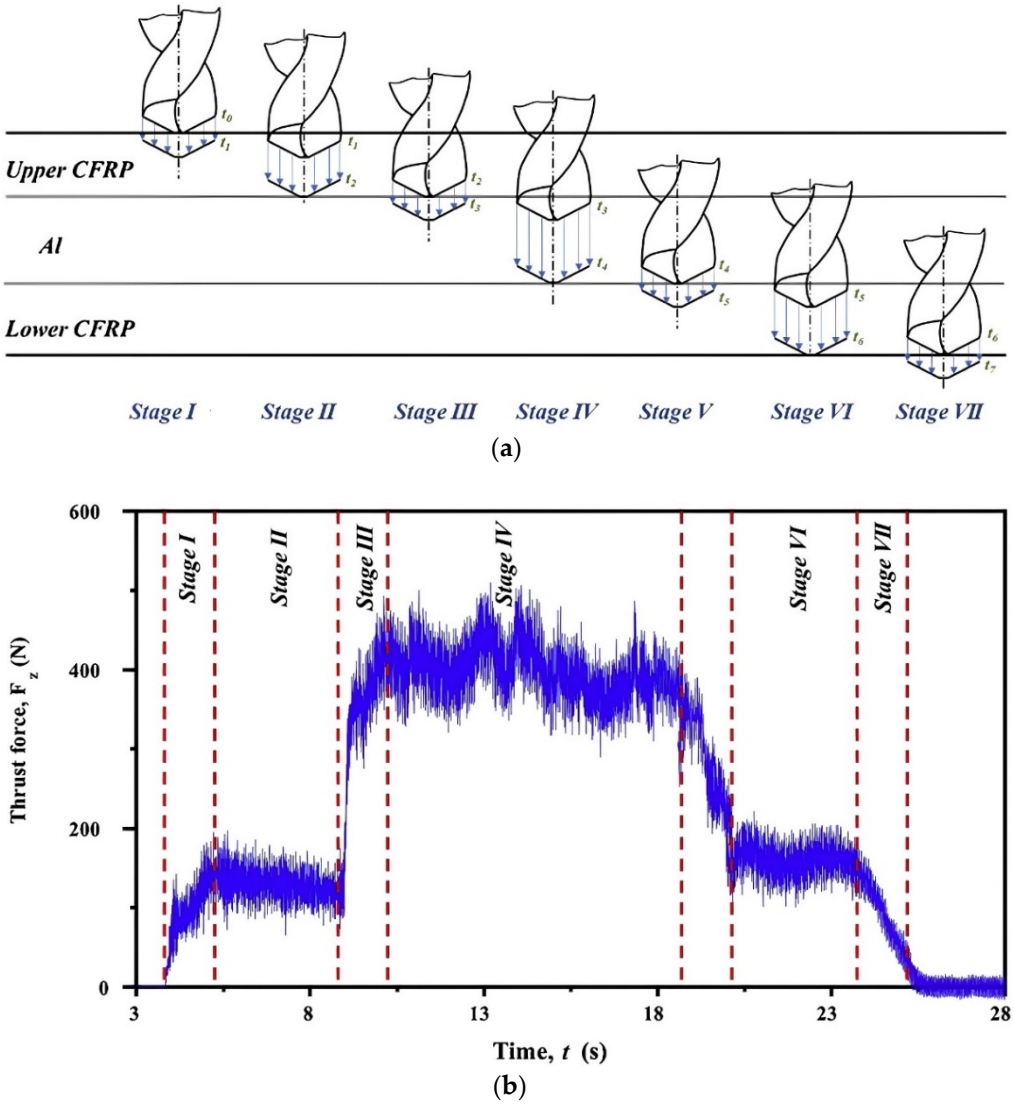

Figure 8. Drilling of CFRP/Al/CFRP co-cured materials: (**a**) stage division of the drilling process and (**b**) thrust force evolution as a function of cutting time [110].

Cutting forces can be measured using a dynamometer or a cutting force sensor or by obtaining cutting force values based on various machining factors, such as tool deflection or vibration [130]. However, during the drilling of multilayer fiber-reinforced polymer composites and aluminum stacks, the thrust force and torque components are typically monitored using a piezoelectric Kistler® dynamometer connected to a charge amplifier for converting the resulting charge signals to voltage [7,8,49,77,83,87,92,93,95,97,98,102,103,106,109,110,112,125,127,128,131–137].

2.6. Drilling Temperatures

The improvement of the drilled-hole quality of hybrid composite stacks and FML composites can be ensured thanks to a better understanding of the physical mechanisms involved in one-shot drilling operations. Thus, online parameters, particularly drilling temperatures, need to be monitored to observe their effect on the drilling performance of aerospace assemblies. The investigation of drilling temperatures is even more noticeable, as the drilling of multi-material stacks is usually carried out in dry conditions since the use of cutting fluids is uneconomical and environmentally unfriendly due to the heavy pollution of the CFRP's powdery chips [77].

Wang et al. [87] were the first to provide the evolution of drilling temperatures, plotted as a function of drilling depth, measured during a single-shot drilling operation of a CFRP/Al stack. In this study, an 8.74 mm thick T800-X850 CFRP comprising 46 unidirectional plies laid up in different fiber directions was stacked with 6 mm thick aluminum AA7075-T651 and drilled in dry conditions using a diamond-coated cemented carbide drill, similar to a twist drill but with double point angles at the drill tip. An analogous thermal signature was also found by Dang et al. [137] during the drilling of a co-cured specimen composed of 10 mm thick aluminum AA7050 between two 5 mm thick M30/AG80 CFRPs. The experiments were performed with a TiAlN-coated cemented carbide tool with a point angle of 140° and a helix angle of 30° in dry conditions. As explained previously, cutting forces sharply increase when the chisel edges of the cutting tool start to penetrate the upper CFRP layer. When the chisel edges are fully engaged in the composite material, the cutting forces reach a threshold, which remains constant until the tool tip begins to penetrate the lower aluminum plate. Wang et al. [87] found that this first step of the drilling of a CFRP/Al stack causes a sharp increase in temperature until a maximum value is achieved near the end of the drilling of the CFRP part. This thermal behavior can be attributed to the abrasive nature of carbon fibers and tool wear, which generate large amounts of cutting heat and friction heat during the drilling of CFRPs. When both CFRP and aluminum layers are drilled simultaneously, a sharp rise in thrust force is associated with a sudden fall in temperature, which gradually evolves during the entire drilling process of the aluminum part. This specific evolution of thermal behavior can be attributed to differences in the thermal conductivity properties of the two drilled materials. Indeed, aluminum alloys are known for their high thermal conductivity, which can easily evacuate the excessive temperature built up during the drilling of the top CFRP layer. The authors explained that the chosen cutting parameters induce the generation of long and flexible metal chips, which accumulate and tangle around the drill bit. Therefore, the friction heat generated by the scraping of aluminum chips on the hole wall surface results in an increase in the drilling temperature. Wang et al. [87] also showed that the increase in feed rate generated fragmented metal chips, and thus, no rise in temperature was observed when the tool tip reached the hole exit of the lower aluminum layer. Finally, the emergence of the chisel edges from the aluminum layer at the end of the drilling process results in a gradual decrease in the drilling temperature at ambient air temperature. However, as shown in Figure 9, Sato et al. [138] observed a different evolution of the cutting temperature during the drilling of a multi-material stack composed of 5 mm thick CFRP comprising 20 cross-plies and 5 mm thick aluminum AA5056 with a multicoated (TiN-AlN) twist drill with a point angle of 140°, while the thrust force evolution is in keeping with the well-known results of the literature discussed previously in the Section "Drilling forces". The spindle speed chosen in this study is 900 rpm, lower than that used by Wang et al. [89] in their experiments (i.e., 2000 rpm). Moreover, Sato et al. [138] carried out multi-material stack drilling with a feed rate of 0.01 mm/rev, while Wang et al. [87] chose a value of 0.02 mm/rev for this cutting parameter. In these conditions, more cutting heat is generated since a smaller feed rate results in more abrasive friction during the drilling of the CFRP layer and generates more long and non-fragmented metal chips, which are very difficult to evacuate.

Among the existing techniques usually chosen for monitoring the cutting temperatures during machining CFRP [139–142], metal alloys [143–145] and CFRP/Ti [138,142–144,146–153], thermographic and thermocouple methods are the ones commonly preferred for measuring cutting temperatures during the drilling of CFRP/Al stacks [87,93,106,109,110,137,138,154] and FML composites [102,128,155].

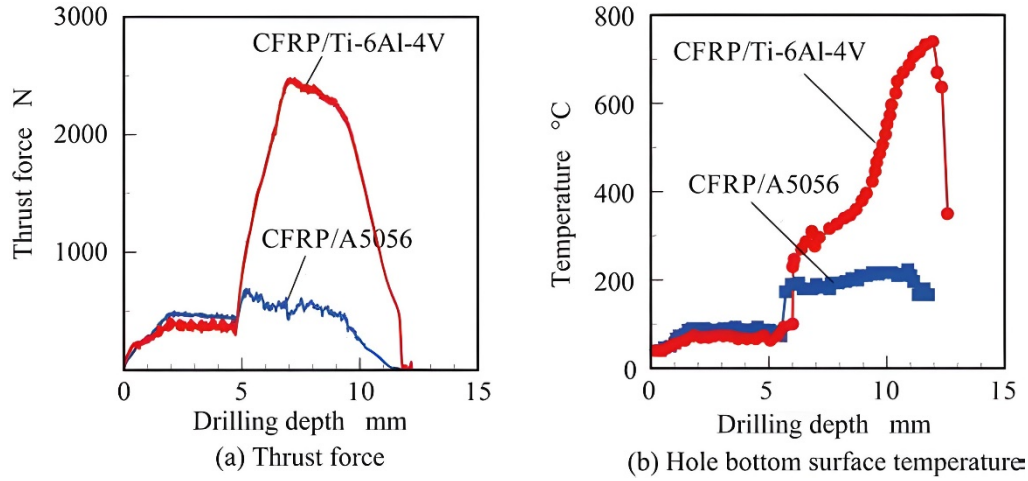

Figure 9. (**a**) Thrust force and (**b**) drilling temperature evolution as a function of drilling depth during the drilling of CFRP/Al and CFRP/Ti stacks [138].

2.7. Tool Wear

Tool wear is commonly considered one of the critical issues that may significantly affect drilled-hole quality, manufacturing costs and the efficiency of the drilling process of multi-material stacks, particularly CFRP/Al stacks and FML composites. Therefore, it is essential to monitor this factor in order to identify the main wear mechanisms occurring during drilling operations, which are responsible for the deterioration of tool life and can lead to catastrophic tool failure. As illustrated in Figure 10, various types of wear can be observed on the cutting tool after drilling both composites and metal materials. Flank wear and, to a lesser extent, crater wear are the generally used main mechanisms of tool wear. Flank wear results from the friction of the tool flank on the drilled-hole wall surface, while the friction of the chip on the tool rake face generates crater wear. More specifically, the most prominent wear mechanisms caused by the drilling of CFRPs are abrasive wear, which is due to the abrasive nature of the carbon fibers, and tool edge chipping [132,156,157]. On the contrary, adhesion wear, diffusion and built-up edge (BUE) are the main wear mechanisms affecting cutting tools when drilling aluminum alloys [7]. BUE is an irregular and unstable structure formed by the successive deposition of material on the tool–chip interface [158]. This tool wear occurs on the tool rake face at low cutting speeds (less than 25 m/min) and acts as a new cutting edge, while chemical action diffusion is favored in severe cutting conditions (greater than 300 m/min) since the temperature becomes higher [159,160]. Furthermore, the wear mechanisms occurring in CFRP/Al stack drilling appear to be a combination of interrelated wear phenomena specific to the drilling of each material separately, i.e., abrasive wear and adhesion wear [3].

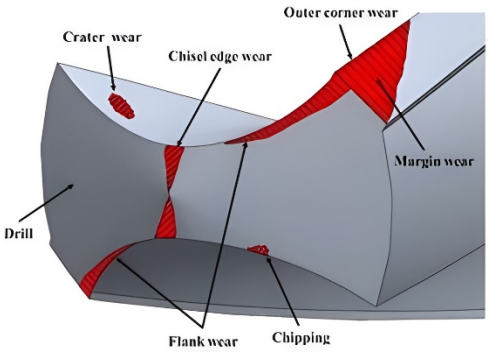

Figure 10. Types of wear on the drill [161].

In practice, tool wear phenomena are analyzed by the Scanning Electron Microscopy (SEM) analysis of cutting tools after drilling. Zitoune et al. [7,90] studied tool wear mechanisms caused by the dry drilling of multi-material stacks with uncoated and nano-coated tungsten carbide drill bits. Experiments were performed on a multi-material stack composed of 4.2 mm thick T700-M21 CFRP (16 plies) and 3 mm thick aluminum AA2024. Regardless of the drill bit (i.e., uncoated or coated), the presence of a layer of aluminum was observed on the cutting edges (BUE), the rake face and the tool flutes (BUL). Moreover, the aluminum–cutting edge interface can be exclusively attributed to mechanical adhesion since no diffusion or oxidation was observed by the authors. Therefore, it can be concluded that the use of coatings did not prevent adhesion wear on the cutting edges. Fernández-Vidal et al. [124] also found that adhesion wear predominated over abrasion of the uncoated cemented carbide twist drill, with a double-angle tip (140°–118°) used for drilling a multi-material stack composed of 4.5 mm thick M21/T800S-24K CFRP comprising 16 plies and 4.86 mm thick aluminum AA7075-T6. Montoya et al. [49] also investigated the wear mechanisms of coated and uncoated tungsten carbide drills with a 124° point angle and 30° helix angle when drilling multi-material stacks composed of 7 mm thick CFRP and 14 mm thick AA7010. Contrary to Zitoune et al. [90] and Fernández-Vidal et al. [124], Montoya et al. [49] found mostly signs of abrasion wear on the drill cutting edges, although some adhesions of aluminum were also present on the tool rake face. This difference in wear phenomena observed in these two distinct studies can be attributed to the use of lower cutting speeds in the investigation performed by Montoya et al. [49]. Indeed, according to List et al. [159], adhesion is favored when machining soft materials such as aluminum at low cutting speeds.

Flank wear assessment is quantified by the value of its width, denoted by V_B. This length located between the current cutting edge and the last point worn on the flank face is generally measured using a toolmaker microscope coupled with a digital camera, especially for CFRP/Al stack drilling [49,88,103,123,125]. However, when a combination of flank wear and edge rounding occurs, local wear quantity *LWQ*, obtained by comparing the current profile of the cutting edge to that of the unworn tool, was proven to be a more appropriate parameter for describing tool wear [49,162].

2.8. Chip Formation

The investigation of chip morphology constitutes a supplementary step for a better understanding of the hole quality, tool wear or cutting forces induced by the drilling of hybrid composite stacks and FML composites. Chip removal issues can be considered among the main challenges in the drilling of CFRP/Al stacks since they affect the drilled-hole wall surface. Indeed, the generation of non-fragmented chips in the aluminum part involves the rolling up of these chips around the drill bit, which can undermine the geometrical and dimensional characteristics of the composite hole when this material is positioned above the aluminum layer when drilling CFRP/Al stacks. The size and shape of chips are impacted by the cutting parameters and cutting tool during the single-shot drilling process. Unfortunately, cutting conditions are quite different between the composite and metal in terms of chip formation during the single-shot drilling process [95]. The formation of fragmented metal chips is required to facilitate their evacuation and thus avoid the deterioration of the drilled-hole surface roughness, while the generation of continuous chips is desirable in the drilling of composite materials since powder-like chips abrade the surface quality [163]. However, such composite chips are difficult to generate because multilayer fiber-reinforced polymer composites are composed of layers that create dust-type chips [164]. Moreover, polymer composite chips are continuous at low feeds, corresponding to cutting conditions that also generate long and non-fragmented chips when drilling the aluminum part [165].

In the scientific literature, several researchers have observed chip morphologies for CFRP/aluminum stacks [77,90,92,95,98,134,166] or FML composites [102,128] using an optical microscope. Zitoune et al. performed dry, single-shot drilling tests with uncoated [90,92]

and nano-coated [90] tungsten carbide drill bits in sandwich plates composed of 4.25 mm thick T700-M21 CFRP (16 plies) stacked with 3 mm thick aluminum AA2024. They found that, regardless of the used type of drill, the shape and size of the chip in the drilling of aluminum were clearly impacted by the choice of feed rate, while the choice of cutting parameters showed no influence on the chip morphology in the drilling of CFRP. According to the previous work of Kim and Ramulu [165], Zitoune et al. [90,92] found that aluminum chips, which were long and continuous at a low feed rate (0.05 mm/rev), became fragmented when increasing the feed rate (0.15 mm/rev). El Bouami et al. [134,166] showed that the drill geometry design affected aluminum chip formation when drilling CFRP/Al stacks. In particular, the use of a step twist drill resulted in small chips in the first step and long chips in the second one, which the authors attributed to the fact that the secondary step of the tool acted as a reaming tool. Hassan et al. [77,95,98] conducted several studies on the single-shot dry drilling of a multi-material stack composed of 3.587 mm thick CFRP—26 plies of unidirectional carbon fiber and 2 plies of glass fiber, which were placed at the top and bottom of the laminate—and 3.317 mm thick aluminum AA7075-T6. Drilling tests were carried out by using an advanced electronic pneumatic drilling unit [95] or a high-speed CNC milling machine [77,98] with uncoated customized tungsten drill bits with various values of point angle, helix angle, primary clearance angle and chisel edge angle. Contrary to Zitoune et al. [90], they found that the carbon dust characteristics differed depending on the tool geometry parameters and feed rate, as depicted in Figure 11. Moreover, regardless of the tool geometry and cutting parameters, the aluminum chips produced during multi-material stack drilling were long and continuous, as shown in Figure 12. This is consistent with the results of Zitoune et al. [90] since fragmented aluminum chips were only observed from a feed rate of 0.15 mm/rev, whereas Hassan et al. [95,98] performed their drill tests with feed rates lower than 0.1 mm/rev.

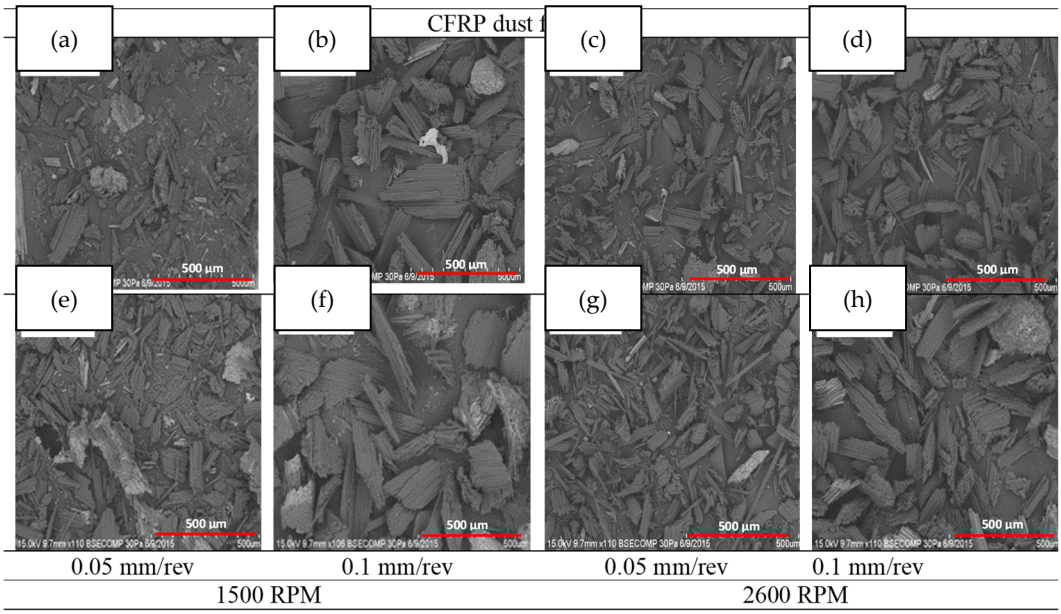

Figure 11. Dust characteristics of CFRP depending on tool geometry parameters and cutting parameters: (**a**–**d**) Point angle of 110°, (**e**–**h**) Point angle of 130° [95].

Sridhar et al. [128] and Bolar et al. [102] observed the same tendencies concerning the evolution of the aluminum chip morphology with the feed rate when drilling CARALL FML, composed of carbon fiber prepreg and AA2024 aluminum layers stacked alternately, using a 6.8 mm diameter solid carbide two-fluted drill with a 140° point angle. However, spindle speed was also found to influence the chip breakability, although its impact was considerably lower than that of the feed rate.

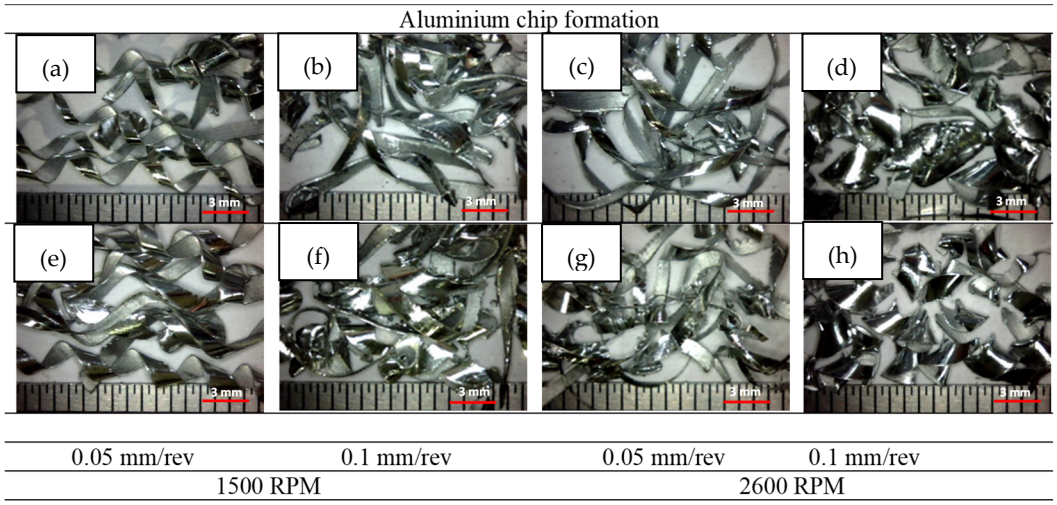

Figure 12. Chip characteristics of AA7075-T6 depending on tool geometry parameters and cutting parameters: (**a**–**d**) Point angle of 110°, (**e**–**h**) Point angle of 130° [95].

3. Optimization of Strategies for High-Performance Drilling of Multi-Material Stacks

High-performance drilling of multi-material stacks is a challenging task in the modern aviation industry, since alternative criteria of drilled-hole quality are expected for each stacked constituent. Hole defects induced by the drilling of CFRP/Al stacks and FML composites include delamination, fiber breakage and hole wall damage due to metal chip transport through the FRP layer, exit burrs in the aluminum layer and hole size and geometrical errors in both constituents. Therefore, the suppression of exit burrs and minimum drilled-hole wall surface roughness are commonly required to achieve satisfactory hole quality for the aluminum layer, whereas drilling-induced delamination elimination and control of hole size and geometrical accuracy represent the preferred criteria for high drilled-hole quality in the composite layer. Various approaches based on an appropriate selection of cutting parameters, cutting tool and cutting environment are suggested in the scientific literature in order to improve the single-shot drilling operation for multilayer fiber-reinforced polymer composites and aluminum stacks and to meet the stringent requirements of the aerospace industry for drilled-hole quality. Hence, the following sections provide an extensive review of the most recent investigations and developments of high-performance drilling of FRP/Al stacks and FML composites, focusing on the influence of the cutting parameters, cutting tool and cutting environment on drilled-hole quality.

3.1. Selection of Cutting Parameters

In a drilling process, cutting parameters include spindle speed and feed rate. Spindle speed, which is denoted by N and expressed in revolutions per minute (rpm), represents the rotational speed of the drill bit. It is related to cutting speed V_c (in m/min), defined as the relative velocity between the surface of the workpiece and the cutting tool. Feed rate, which is denoted by f and expressed in mm/rev, is the distance traveled during one complete revolution of the drill bit. The linear travel rate (in mm/min) of the cutting tool can be calculated by multiplying f by N. Cutting parameters are commonly considered prominent parameters in the drilling of hybrid composite stacks since they directly impact delamination, hole surface roughness, dimensional accuracy, burr formation, drilling forces, thermal aspects, tool wear and chip formation and thus determine the drilling performance of aerospace assemblies. Over the last decade, much research on the influence of drilling parameters on the overall drilling performance have been carried out on various stacking sequences, such as CFRP/Al [7,83,87,88,90,95,97,103,109,125,134,166–168],

CFRP/Al/CFRP [8,117,137], Ti/CFRP/Al [12], CFRP/GFRP/Al [97], Al/GFRP/Al [106,112] and FML [78,99,102,105,128,129,169–171].

Zitoune et al. [7] studied the influence of spindle speed (1050, 2020 and 2750 rpm) and feed rate (0.05, 0.10 and 0.15 mm/rev) on cutting forces (thrust force and torque components), hole surface roughness and chip morphology when drilling T700-M21/AA2024 stacks (4.2/3.0 mm thick) with 4, 6 and 8 mm diameter uncoated tungsten carbide drill bits. They noted that the magnitude of cutting forces during the drilling of the aluminum constituent compared to the CFRP constituent was affected by the feed rate, varying from double at a low feed rate (0.05 mm/rev) to triple at a higher feed rate (0.1 and 0.15 mm/rev). Moreover, variation in the feed rate significantly influenced cutting forces, metal chip morphology and drilled-hole wall roughness, while the choice of spindle speed showed a negligible effect. Therefore, a feed rate lower than 0.1 mm/rev seemed suitable to generate small fragmented aluminum chips, which limited the deterioration of the drilled-hole surface roughness in the CFRP layer. Indeed, rougher surface finishes (R_a ~ 6–8 µm) were found at a high feed rate compared to those at a lower feed rate (R_a ~ 2–4 µm). Then, Krishnaraj et al. [167] investigated the influence of spindle speed, feed rate and drill diameter—and their interactions—on the overall performance when drilling T700-M21/AA2024 stacks (4.2/3.0 mm thick) under the same conditions as previously reported [7]. The analysis of variance (ANOVA) confirmed that the feed rate and drill diameter had a more dominant effect on cutting forces and on the surface roughness of each constituent of the CFRP/Al stack than spindle speed. In [7,167], the hole diameter on CFRP was found to be 10 µm less than the nominal diameter of the drill, and the authors of these studies attributed this phenomenon to the cutting edge radius of the cutting tool and the relaxation of elastic stresses during the drilling process. Moreover, they found that circularity error worsened with the increase in feed rate, varying from 6 µm at 0.05 mm/rev to 25 µm at 0.15µm. Zitoune et al. [90] further reported the effect of cutting parameters on the drilling performance by completing the previous study [7] through a comparison with the results of experiments carried out on the same multi-material stack with a nano-coated tungsten carbide drill bit. From this experimental study, the selection of a nano-coated tool with a spindle speed of 2020 rpm and a feed rate of 0.1 mm/rev was found to produce fragmented chips, reduce thrust forces in each constituent of the CFRP/Al stack, significantly enhance the surface roughness and thus improve the drilling performance compared to uncoated drills. Similarly, Wang et al. [87] considered the influence of spindle speed (1000, 2000 and 3000 rpm) and feed rate (0.02, 0.04, 0.06 and 0.08 mm/rev) on thrust force, drilling temperature, hole diameter and surface roughness when drilling T800-X850/AA7075-T651 stacks (8.74/6.00 mm thick) with a 9.53 mm diameter diamond-coated cemented carbide double cone drill bit (first point angle: 130°; second point angle: 60°) in dry conditions. In accordance with the study of Zitoune et al. [7], they also found that the thrust force recorded during the drilling of the aluminum constituent was about two times higher compared to that recorded during the drilling of the CFRP constituent. In addition, the thrust force in each constituent of the CFRP/Al stack was almost proportional to the feed rate, whereas spindle speed had no significant effect. The surface roughness of the CFRP hole wall was found to increase slowly with increasing feed rate. Although the drilling experiments performed by Zitoune et al. [7] showed that variation in the feed rate significantly influenced drilled-hole wall roughness, it is important to note that this tendency was not observed for the same range of feed rates (from 0.05 to 0.15 mm/rev). Moreover, the values of surface roughness R_a found by Wang et al. [87], which varied from 2 to 3 µm at the chosen range of feed rates (from 0.02 to 0.08 mm/rev), are consistent with the results (R_a ~ 2–4 µm) found by Zitoune et al. [7] for feed rate values of 0.05 and 0.1 mm/rev. Wang et al. [87] also investigated the influence of drilling parameters on the diameter difference. They reported that the hole diameter of each constituent of CFRP/Al increased with the feed rate. Moreover, the Al hole was always smaller than the CFRP hole, and smaller diameter tolerance between CFRP and Al holes could be achieved at higher spindle speed. The measurement of drilling temperature during the drilling of CFRP/Al stacks

showed that a lower maximum drilling temperature could be achieved with lower spindle speed and a larger feed rate. Indeed, it was found that the drilling temperature increased with the increase in spindle speed or the decrease in feed rate due to the improvement of the abrasive wear of the cutting tool and the extension of the drilling time in these machining conditions. Similar results were found by Dang et al. [137] when drilling co-cured M30-AG80/AA7050 with various cutting speeds (30, 60, 90 and 120 m/min) and feed rates (0.01, 0.02 and 0.03 mm/rev) using a 6 mm diameter TiAlN-coated cemented carbide twist drill bit with a 140° point angle and a 30° helix angle. Zhang et al. [88] examined the impact of higher spindle speeds (2700, 3500, 4300, 5100 and 5900 rpm) and feed rates (0.03, 0.04, 0.05, 0.06 and 0.07 mm/rev) on the cutting forces and hole diameter when drilling CCF300/AA7075-T7 stacks (3.07/3.10 mm thick) with two different geometries of a 5 mm diameter diamond-coated cemented carbide twist drill bit in dry conditions. They found that variation in spindle speed had no further effect on cutting forces, regardless of tool geometry, whereas they increased when varying the feed rate, which is consistent with the aforementioned results at spindle speeds lower than 3000 rpm. In contrast, the diameter of the drilled hole in the CFRP layer became larger when increasing spindle speed, more significantly with a conventional twist drill, whereas the feed rate had little effect, regardless of the cutting tool used. Hassan et al. [95] studied the influence of spindle speed (1500 and 2600 rpm) and feed rate (0.05 and 0.10 mm/rev) on hole diameter, hole surface roughness and aluminum burr height when drilling CFRP/AA7075-T7 stacks (3.587/3.317 mm thick) using 4.826 mm diameter uncoated tungsten carbide twist drill bits with various geometry parameters (point angle, helix angle, chisel edge angle and primary clearance angle) in dry conditions. They noted that all of these outputs were impacted by variations in both spindle speed and feed rate, except for the diameter difference between CFRP and Al holes, which was not much affected by the chosen feed rate. Indeed, a decrease in both spindle speed and feed rate resulted in smoother CFRP hole roughness but higher metal burr height at the exit hole. Moreover, hole diameter difference was improved when drilling at lower spindle speed. As burr height is related to the engagement time of tool–workpiece interaction, it is preferable to minimize this time by increasing drilling parameters in order to reduce the heat generated at the drill bit during the drilling process and thus produce smaller burrs. From this study, Hassan et al. [95] concluded that the best hole quality of CFRP/Al stacks, characterized by the achievement of the minimum difference in diameter, the minimum hole surface roughness and the minimum burr height formation, could be achieved with a spindle speed of 2600 rpm and a feed rate of 0.1 mm/rev using a drill bit with the optimal combination of a helix angle of 15°, primary clearance angle of 8°, point angle of 130° and chisel edge angle of 30°. Banon et al. [96] carried out ANOVA analysis and response surface methodology (RSM) in order to identify the influence of cutting speed (85, 115 and 145 m/min) and feed speed (200, 250 and 300 mm/min) on the hole diameter and hole surface roughness when drilling CFRP/AA2024 stacks (2/8 mm thick) with a 7.92 mm diameter uncoated carbide double cone drill bit (first point angle: 140°; second point angle: 118°) in dry conditions. The lowest value of R_a in the CFRP layer was obtained by combining a lower cutting speed and lower feed speed, which is consistent with the conclusions of Hassan et al. [95]. Moreover, it was found that drilling parameters did not influence the diameter deviations obtained by the ANOVA analysis, which the authors attributed to their randomness as a consequence of secondary adhesion wear. Bayraktar and Turgut [168] also performed ANOVA and RSM in order to identify the impact of cutting speed (100, 125 and 150 m/min), feed rate (0.1, 0.2 and 0.3 mm/rev) and point angle (90, 118 and 135°) on delamination occurrence in the hole entrance and exit when drilling CFRP/AA6013-T651 stacks using 8 mm diameter uncoated and TiN- and TiAlN-coated HSS drills with a 30° helix angle. The most effective parameters on the hole entrance and exit delamination of the CFRP constituent were determined, respectively, as the feed rate, followed by the drill point angle and cutting speed. A reduction in delamination extent was observed when increasing the cutting speed or decreasing the feed rate when drilling multi-material stacks with uncoated tools. The rise in drilling temperature based

on cutting speed involves softening of the matrix phase of CFRP and thus facilitates the cutting process, whereas chip formation resistance increases with the feed rate. Therefore, the statistical analysis showed that the highest cutting speed combined with the lowest feed rate was considered the optimal set of cutting parameters in terms of the delamination factor for uncoated drills with the lowest angle point. The influence of high cutting speeds (59, 119 and 178 m/min), which are comparable to the spindle speeds used by Zhang et al. [88], and feed speeds (9, 15 and 21 mm/min) on thrust force and hole quality was investigated by Mahdi et al. [83] when drilling AS4-M26T/AA2198 stacks (4.6/3.0 mm thick) using a 6.3 mm diameter uncoated carbide twist drill bit with a 120° point angle and 30° helix angle in dry conditions. Hole damage was estimated using the delamination factor F_d and macroscopic observations of the interior and exterior of drilled holes in both CFRP and aluminum constituents. Regardless of the cutting parameters, exit delamination was always higher than entry delamination of the CFRP layer. The delamination factor rose when increasing feed speed, whereas cutting speed had a negligible effect on the value of F_d. In addition, macroscopic observations of the hole showed that the occurrence of drilling defects, such as uncut fibers, chipping and spalling in the CFRP layer, were mainly influenced by cutting speed. Contrary to other studies cited above [7,87,89,167], cutting speed was found to be the most prominent factor influencing thrust force compared to feed speed. These results can be attributed to the choice of very low feed speeds (corresponding to feed rates from 0.001 to 0.002 mm/rev) in comparison with the range of feed rates commonly found in the scientific literature. Moreover, the use of higher cutting speeds implies an increase in cutting edge temperature during the process, which reduces the cutting resistance of aluminum and CFRP and thus results in a decrease in thrust force on both materials.

Research on FML drilling has been scarce over the last decade. The main purpose of these studies, dedicated to glass laminate aluminum-reinforced epoxy (GLARE) [78,99,129,169,171] and carbon-reinforced aluminum laminate (CARALL) [102,105,128,170], is to identify the best process parameters in order to meet the industrial requirements concerning the drilled-hole quality of these specific composite materials. In particular, several authors considered the influence of cutting parameters on thrust force [78,102,128,129,169–171], roughness [78,102,128,129,170], dimensional error [99,102,105,128,129,169], burr formation [99,102,128,169,171] and delamination [99,105,169,170].

Pawar et al. [169] addressed the understanding of cutting mechanisms during the drilling of GLARE by investigating the effect of high spindle speeds (4500, 600 and 7500 rpm) and feed rates (0.15, 0.225 and 0.3 mm/rev) on cutting forces, delamination and hole size variations. Drilling experiments were performed on two grades of alternating thin layers of aluminum and GFRP composites, namely, GLARE 5 and GLARE 6, using 6.35 mm diameter uncoated solid carbide twist drill bits with a helix angle of 30°, a point angle of 120° and four different drill point geometries (i.e., two-fluted, three-fluted, four-faceted and eight-faceted drills). They reported that cutting forces increased with the feed rate, regardless of the drill point geometry. In contrast, the variation in cutting forces was found to be relatively low regardless of the variation in spindle speed. In particular, cutting forces decreased at spindle speeds higher than 6000 rpm. This phenomenon can be attributed to the softening of aluminum and the matrix caused by higher cutting temperatures. No delamination was observed using two-fluted and four-faceted drills. For the two other drill point geometries, the value of the delamination factor increased with the feed rate, while its evolution showed a similar trend to that of cutting forces when spindle speed increased. Moreover, the four drill point geometries produced slightly undersized holes because of the relaxation of elastic stresses due to different elastic moduli and coefficients of thermal expansion of drill and work materials. Giasin et al. [78] investigated the influence of spindle speed (1000, 3000, 6000 and 9000 rpm) and feed speed (100, 300, 600 and 900 mm/min) on cutting forces and surface roughness when drilling three different grades of GLARE panels, namely, GLARE 2B 8/7-0.4 (5.113 mm total thickness), GLARE 2B 11/10-0.4 (7.130 mm total thickness) and GLARE 3 8/7-0.4 (5.113 mm total thickness), using a 6 mm diameter coated

carbide drill. They reported that feed speed and spindle speed had a significant impact on cutting forces, which can be reduced by decreasing feed speed or increasing spindle speed. In addition to this, an ANOVA analysis showed that the contribution of spindle speed (~58%) was more important than that of feed speed (~35%) on cutting forces, while the influence of their interaction was much lower (~6%). The cutting parameters also had an influence on the average roughness R_a of the overall combination of aluminum sheets and S2/FL94 layers. Indeed, the drilled-hole wall surface roughness became smoother when decreasing spindle speed or feed speed. The ANOVA analysis showed that the contributions of both cutting parameters were similar when drilling GLARE 2B, regardless of the total thickness, while surface roughness was more impacted by spindle speed than feed speed when drilling GLARE 3. Furthermore, fiber orientation in GLARE grades had an influence on surface roughness, whereas its impact on cutting forces was negligible. Indeed, the drilled-hole surface roughness of GLARE 2B (layers with the same fiber orientation) was smoother than that of GLARE 3 (layers with different fiber orientations). Finally, the authors recommended coupling low feed speed (100 mm/min) with low or moderate spindle speed (1000–3000 rpm) in order to achieve minimum roughness, better surface finish and good hole quality, whereas cutting forces could be minimized when drilling with higher spindle speed (9000 rpm). Giasin and Ayvar-Soberanis [99] further studied the contribution of cutting parameters to burr formation and hole size when drilling the same grades of GLARE panels used in [78] with the same ranges of spindle speed and feed speed. They reported that the height and thickness of burrs at both the entrance and the exit of the hole increased with feed speed, while the impact of spindle speed on this defect was dependent on feed speed. However, the ANOVA analysis allowed them to identify spindle speed as the most influential parameter on burr formation, followed by feed speed and the interaction between them. In addition, the authors suggested that fiber orientation in GLARE grades had an influence on hole size since the reduction in hole size in GLARE 3 (layers with different fiber orientations) at the bottom was greater than that in GLARE 2B (layers with the same fiber orientation). Oversized holes were produced at the top location, while undersized holes were measured at the bottom location. The diameter of the hole at the bottom was reduced by increasing spindle speed, while the hole size at the top became larger. The influence of a large range of spindle speeds (2000, 3000, 4000, 6000, 8000, 10,000, 12,000, 14,000, 16,000 and 18,000 rpm) and feed rates (0.02, 0.04, 0.08, 0.15, 0.18, 0.25 and 0.3 mm/rev) on the drilling performance of GLARE 2B 11/10-0.4 (7.130 mm total thickness) was analyzed by Bouhdiri et al. [129]. Drilling experiments were performed using 6 mm diameter uncoated and coated (DLC- or diamond-coated) cemented carbide twist drills. In accordance with most studies on the drilling of hybrid composite stacks and FML composites, the authors pointed out that cutting forces increased with the feed rate for all tools. In addition, increasing the feed rate did not affect the circularity of the drilled holes, but the circularity error of the holes increased with increasing spindle speed. Moreover, it revealed that spindle speed did not have the same impact on thrust force and torque. Indeed, although spindle speed had an insignificant effect on thrust force, the variation in torque differed depending on the range of spindle speeds. In detail, the influence of spindle speed on torque was first negligible up to 4000 rpm. This result is consistent with the results found in research articles with similar spindle speeds, and it can be attributed to the temperature caused by drilling, which is not high enough to affect the mechanical properties of the GLARE composite. When spindle speed increased to 14,000 rpm, torque decreased. Pawar et al. [169] observed the same phenomenon at spindle speeds higher than 6000 rpm and assumed that this evolution could be attributed to the softening of aluminum and the matrix caused by higher cutting temperatures. At spindle speeds greater than 14,000 rpm, Bouhdiri et al. [129] reported that torque increased sharply, which could be explained by the increased vibration of the cutting tool due to the dynamic effects of the drilling process. Recently, Bonhin et al. [171] investigated the influence of spindle speed (4000 and 8000 rpm) and feed rate (0.05, 0.10 and 0.15 mm/rev) parameters on thrust force and burr height when drilling GLARE material (AA2024-T3/glass fiber-

reinforced epoxy) using a 4.8 mm diameter TiAlN-coated twist drill with a point angle of 140° and a helix angle of 30°. The ANOVA analysis of these results showed that the feed rate was the main contributing factor (99.75%) affecting thrust force. The authors reported that thrust force and burr thickness increased with the feed rate, regardless of spindle speed. The feed rate contributed the most (63.14%), followed by spindle speed (27.59%), to influencing burr thickness. In addition, it had a noticeable impact (21.33%) on burr height, although its interaction with spindle speed was the largest contributing factor (75.76%). According to the results of this study, burr formation could be minimized by drilling at a low spindle speed and feed rate. Finally, the authors recommended the use of a spindle speed of 4000 rpm with a feed rate of 0.05 mm/rev in order to minimize thrust force and burr formation.

Very recently, Ekici et al. [170] examined the influence of cutting speed (65, 85 and 110 m/min) and feed rate (0.10, 0.14 and 0.20 mm/rev) on thrust force, surface roughness and delamination and hole quality during the drilling of a CARALL composite composed of four layers of CFRP and three layers of AA5754 (5 mm total thickness). Drilling experiments were performed in dry conditions using 6 mm diameter uncoated and signum-coated carbide twist drill bits with a helix angle of 30° and a point angle of 118°. The ANOVA analysis showed that the feed rate was the most effective drilling parameter, with a 93.87% contribution ratio, which is comparable to that found by Bonhin et al. [171] for GLARE material. No significant effect was found for cutting speed (0.73%). Surface roughness was found to be controlled by the coating–cutting speed interaction, with a 66.504% contribution ratio, followed by cutting speed (9.551%). Delamination seemed to be similarly impacted by coating, cutting speed and the cutting speed–feed rate interaction (29.13, 24.61 and 21.52%, respectively). The authors used hybrid gray relational analysis–principal component analysis (GRA-PCA) multi-objective optimization, and the optimal values of cutting parameters were recommended as a cutting speed of 110 m/min and a feed rate of 0.1 mm/rev to achieve the minimum thrust force, surface roughness and delamination when drilling CARALL using an uncoated tool. Ekici et al. [105] further investigated the effect of cutting parameters on hole size by completing the previous study [170] with a comparison with results from experiments carried out on the same CARALL with a supplementary nanofiber-coated carbide drill bit. They found that both entrance and exit hole diameters achieved values closer to the nominal hole diameter when increasing the feed rate, which is consistent with the conclusions of Soo et al. [125] for CFRP/Al stacks. In addition, exit drilled holes exhibited smaller diameters than those observed at the top surface of CARALL material, as found by Giasin and Ayvar-Soberanis [99] for GLARE drilling. Sridhar et al. [128] investigated the effect of spindle speed (1000, 2000, 3000 and 4000 rpm) and feed rate (0.1, 0.2, 0.3 and 0.4 mm/rev) on thrust force, drilling temperature, surface roughness, hole diameter and burr size when drilling a CARALL composite composed of seven layers of CFRP (0.2 mm thick by layer) and eight layers of AA2024 (0.5 mm thick by layer). Drilling experiments were performed in dry conditions using 6.8 mm diameter two-fluted solid carbide drill bits with a point angle of 140°. The authors found that spindle speed and feed rate had a significant impact on thrust force, drilling temperature, surface roughness, hole diameter and burr size. In detail, the ANOVA analysis showed that the feed rate, followed by spindle speed, significantly influenced thrust force, surface roughness and burr size, while the cutting temperature and hole diameter were more impacted by spindle speed than the feed rate. Thrust force can be reduced by increasing spindle speed, inducing a rise in the machining temperature and material softening. Thrust force can also be lessened by decreasing the feed rate. Consequently, the minimum thrust force was measured at a spindle speed of 4000 rpm and a feed rate of 0.1 mm/rev. Surface roughness was improved by increasing spindle speed due to reduced BUE formation tendency and smaller chip size. Better roughness can also be achieved by increasing the feed rate because chip evacuation is favored by the formation of very fragmented chips at higher feed rates. Thus, the minimum roughness was achieved at a spindle speed of 4000 rpm and a feed rate of 0.4 mm/rev. Uniform burrs without caps were observed at the periphery of the exit of

the hole, regardless of the cutting parameters. Their height and width were found to be greater with the increase in spindle speed or feed rate. Hence, the minimum burr size was obtained at a spindle speed of 1000 rpm and a feed rate of 0.1 mm/rev. Finally, the authors reported that oversized holes were produced with all of the chosen cutting parameters, and the hole diameter drew near the nominal diameter when increasing spindle speed or feed rate, which seems consistent with the results of Ekici et al. [105]. Moreover, higher spindle speeds and feed rates were recommended to produce holes within H9 diameter tolerance.

3.2. Selection of Cutting Tool

In the single-shot drilling of CFRP/Al stacks and FML composites, tool geometry, as well as tool material and tool coating, considerably alter the overall drilling performance. Hence, the selection of the correct drill bit is just as important as the choice of cutting parameters for drilling high-quality holes and prolonging tool life. However, this remains a major challenge due to the difficulty in designing a cutting tool suitable for both constituents of hybrid composite stacks when they exhibit different wear mechanisms. Additionally, it is necessary to find the best compromise between drilled-hole quality, tool wear resistance and production costs, which can be achieved by using coated tools [49,78,87,88,90,99,104,106,125,129,137,170] and/or special morphologies of drills [48,88,92,94,117,125,134,166].

3.2.1. Tool Material and Coating Type

Various types of tool materials, including high-speed steel (HSS), cemented or tungsten (K10, K20, WC, WC-Co, etc.) carbides or polycrystalline diamond (PCD), may be chosen depending on the drilled material. As explained in detail by Aamir et al. [13,172], the recommended tool materials for drilling composites and aluminum alloys are cemented and tungsten carbides because of their extreme hardness, toughness and wear resistance compared to HSS, even at high temperatures. Therefore, the majority of experimental investigations and studies regarding CFRP/Al stacks and FML composites in the literature were performed using cemented or tungsten carbide tools [7,49,78,83,87,88,90,92,94–96,99–101,104,105,117,125,128,128,134,137,166,167,169–171]. Furthermore, the deposition of a coating layer, which can be performed using physical vapor deposition (PVD) or chemical vapor deposition (CVD) techniques, has proven to be an accepted solution for the improvement of the drilling performance of carbide drills by enhancing their wear resistance and thus extending their life. Over the last decade, several studies have focused on the effect of coatings, including AlTiN/TiAlN [99,104,105,137], TiN [99,105], diamond [87,89,125,129] and diamond-like carbon (DLC) [104,129] coatings, on the overall performance when drilling CFRP/Al stacks and FML composites.

Zitoune et al. [90] investigated the effect of nanocomposite coating-type nanocrystalline-CrAlN/amorphous-Si3N4 (2.32 µm thick) on thrust force, surface roughness, chip shape and tool wear when drilling T700-M21/AA2024 stacks (4.2/3.0 mm thick) at various spindle speeds (1050, 2020 and 2750 rpm) and feed rates (0.05, 0.10 and 0.15 mm/rev) using two variants (uncoated and coated) of 6 mm diameter tungsten carbide drill bits with a 132° point angle. The authors found that the use of nano-coated drills induced a reduction in thrust force, with a more substantial reduction for the aluminum layer (47%) than for the CFRP layer (20–25%), compared to the results recorded when drilling with an uncoated tool under the same cutting conditions. This tendency was attributed to the reduction in friction due to cutting tool–workpiece and chip–flute interactions. Moreover, the use of nano-coated tools enabled a smoother hole wall surface roughness in the CFRP layer to be produced, corresponding to a decrease of 40% compared to the roughness obtained with the uncoated tool, although it was also observed that the coating did not prevent BUE of aluminum on the cutting edges. Montoya et al. [49] studied the performance of three different types of tool coatings (diamond, TiAlCrN and AlTiSiN-G) when drilling CFRP/AA7010-T7451 stacks (7/14 mm thick) using 6 mm diameter tungsten carbide drills with a 124° point angle and a 30° helix angle. Drilling tests were performed in dry conditions at a spindle speed

of 3000 rpm and a feed rate of 0.04 mm/rev, and the evolutions of flank wear, thrust force and hole diameter with the number of drilled holes were compared with experimental results obtained using an uncoated twist drill using the same geometry. They found that TiAlCrN and AlTiSiN-G coatings were inefficient in terms of tool wear prevention, since these coatings suffered delamination starting from the 5th hole and were completely removed from the flank and rake faces after drilling 75 holes. Consequently, the thrust forces generated by these coated tools in both CFRP and Al layers were similar to those measured when drilling the multi-material stack using the uncoated tool, regardless of the number of drilled holes. In contrast, a diamond-coated drill showed the lowest flank wear (about 120 µm) after 250 holes, which was reduced by half compared to that observed with the uncoated tool. The thrust forces generated with this drill bit were found to be significantly reduced (CFRP: 65%; Al: 35%) compared to those obtained with the uncoated tool after a few holes. The contribution of diamond coating to the delay of tool wear showed the best surface roughness (about 0.2 µm *Ra* in Al and 1.2 µm R_a in CFRP) after 250 drilled holes, while the uncoated tool already produced a level of roughness higher than the maximum authorized in the aeronautics industry (3.2 µm R_a in CFRP) starting from the 75th hole. D'Orazio et al. [104] highlighted the tool wear mechanisms occurring when drilling CFRP/AA7075-T651/CFRP stacks (2.8/20.0/2.8 mm thick) using two different 6.8 mm diameter twist drills, including DLC- and nanocomposite TiAlN-coated tools. Drill experiments were performed in wet conditions, with a chip removal cycle consisting of two passes, separated by a back motion required to remove chips. The analysis of SEM images of the worn TiAlN- and DLC-coated tools after 170 holes, when the coating of both TiAlN- and DLC-coated had been almost completely worn and removed, showed that the wear mechanisms were different depending on the type of tool coating. The TiAlN-coated tool was essentially affected by abrasion, with few adhesions of aluminum particles on the rake face of the tool, while chipping was localized in the periphery of the cutting edge, and edge rounding and abrasion were the main wear mechanisms identified when drilling the multi-material stack using the DLC-coated drill bit. Additionally, the TiAlN-coated tool exhibited higher flank wear than the DLC-coated drill bit, the magnitude of which increased with the number of drilled holes. The authors also showed that DLC coating allowed them to achieve a lower delamination factor than TiAlN coating, with a constant gap regardless of the number of holes. Bayraktar and Turgut [168] studied the impact of coating on delamination and optimal cutting parameters when drilling CFRP/AA6013-T651 stacks using 8 mm diameter uncoated and TiN- and TiAlN-coated HSS drills with a 30° helix angle at various cutting speeds (100, 125 and 150 m/min) and feed rates (0.1, 0.2 and 0.3 mm/rev). The authors reported that the uncoated cutting tool produced less delamination than TiN- and TiAlN-coated drill bits, with similar entrance and exit delamination factors for both of these coated tools. This trend can be attributed to the reduction in the sharpness of the cutting edge caused by the deposition of coating, which causes more difficulties for the cutting tool to penetrate the material. The authors determined the optimal cutting parameters depending on the cutting tool. Thus, they found that the entrance delamination factor of the CFRP constituent was minimized when drilling CFRP/AA6013-T651 stacks at the highest cutting speed (150 m/min) and the lowest feed rate (0.1 mm/rev). The same feed rate of 0.1 mm/rev was recommended to minimize the exit delamination factor for all drill bits. However, a cutting speed of 125 m/min was recommended for the uncoated and TiAlN-coated tools, whereas a cutting speed of 150 m/min was required for the TiN-coated tool. Very recently, Zhong et al. [127] focused on the effect of TiAlN coating on thrust force, hole wall surface roughness and delamination when drilling T700-Qy8911/AA2024/T700-Qy8911 co-cured material using 6 mm diameter uncoated and TiAlN-coated drill bits with a 20° helix angle and a 135° point angle at various cutting speeds (15, 30, 45 and 60 m/min) and feed rates (0.025, 0.050, 0.075 and 0.100 mm/rev). The authors found that the maximum thrust force recorded during the drilling of the aluminum constituent was always higher compared to that recorded during the drilling of the CFRP constituent. The performance of the TiAlN-coated tool, in terms of maximum thrust force generated in the Al layer, was

found to be better than that of the uncoated drill bit, whereas the magnitude of maximum thrust force in the CFRP layers was impacted differently depending on the ranges of cutting speeds and feed rates. Indeed, the uncoated tool resulted in a lower maximum thrust force in the CFRP constituent than that produced with the TiAlN-coated tool when drilling at a low cutting speed and feed rate, while this thrust force became greater than that generated by the TiAlN-coated tool with increasing cutting speed, regardless of the selected feed rate. In addition, the use of TiAlN coating improved the drilling performance of the T700-Qy8911/AA2024/T700-Qy8911 co-cured material in terms of delamination since the induced entrance and exit delamination factors were found to be lower using the coated drill bit than when using the uncoated one. By analyzing the SEM images of the hole wall surface in each layer, the authors also found that the TiAlN-coated drill should be recommended for promoting better hole quality.

The impact of the tool material and coating on hole size, delamination and roughness has also been discussed for the drilling of GLARE [100,101,108] and CARALL [105,170] materials. Park et al. [100] focused on the influence of the tool material on average roughness R_a when drilling GLARE 4/3-0.4 at various spindle speeds (600, 1800 and 3000 rpm) and feed rates (0.04, 0.12 and 0.20 mm/rev) using 5 mm diameter HSS-Co and cemented carbide three-fluted twist drills with a 118° point angle and a 25° helix angle. The authors stated that the cemented carbide drill promoted better average roughness and a lower delamination extent than those induced by the HSS-Co cutting tool. They explained that this result could be attributed to the shallower pulling of fibers in the composite layers produced by the cemented carbide drill compared to the results obtained with the HSS-Co cutting tool. Giasin et al. [101] investigated the impact of three types of tool coatings (TiAlN, TiN and AlTiN/TiAlN) on roughness and burr size when drilling GLARE 2B 11/10-0.4 laminate (7.13 mm total thickness) at various spindle speeds (3000, 4500 and 6000 rpm) and feed speeds (300, 450 et 600 mm/rev) using 6 mm diameter coated tungsten carbide twist drills with a 30° helix angle and a 140° point angle. They found that the TiN-coated tool achieved the best average surface roughness of the hole wall, while the TiAlN-coated tool produced the worst, regardless of the cutting parameters. This phenomenon can be attributed to the smaller coefficient of friction associated with the TiN coating compared with that of TiAlN and AlTiN coatings. In addition, the variation in surface roughness between the three tools was more significant when drilling at higher spindle speeds. The ANOVA analysis of the results showed that tool coating, spindle speed and their interactions were the main contributing factors (31.97, 30.44 and 15.98%, respectively) affecting the surface roughness, whereas the feed rate had no impact. The authors also reported that larger burrs were produced at the exit than at the entrance. The tool coating contributed the most to exit burr height and root thickness (71.47 and 62.32%, respectively), while it did not impact the entrance burr height. The three-way interactions between cutting parameters and coating had a significant effect on the entrance burr root thickness, up to 26.02% in three-way interactions, and the tool coating represented the second largest impact (19.28%). Giasin et al. [108] further completed this previous study [103] by investigating the effect of the same tool coatings (TiAlN, TiN and AlTiN/TiAlN) on force thrust and hole accuracy. The authors reported that the AlTiN/TiAlN-coated tool achieved the lowest thrust force and the second highest drilled-hole deviation from the nominal diameter of the tool, while the TiAlN-coated tool produced both the highest thrust force and drilled-hole deviation, regardless of the cutting parameters. This is consistent with the results from [101] concerning the surface roughness obtained with differently coated tools. The authors performed an ANOVA analysis of the results and found that cutting parameters and tool coating contributed almost equally to thrust force. Thus, they concluded that reduced thrust force and limited drilling-induced damage could be achieved thanks to the correct combination of cutting parameters and tool coating. Ekici et al. [105] examined the drilling performance of two types of coatings (TiN-TiAlN and TiAl/TiAlSiMoCr) in terms of hole size and entrance hole delamination. Drilling tests were performed on a CARALL composite composed of four layers of CFRP and three layers of AA5754 (5 mm

total thickness) in dry conditions using 6 mm diameter uncoated and coated carbide twist drill bits with a helix angle of 30° and a point angle of 118° at various cutting speeds (65, 85 and 110 m/min) and feed rates (0.10, 0.14 and 0.20 mm/rev). The authors found that the uncoated tool produced holes with a diameter closer to the nominal diameter than those obtained with the TiN-TiAlN- and TiAl/TiAlSiMoCr-coated tools, certainly due to the sharper cutting edge of the uncoated tool compared to the coated drill bits. The uncoated tool achieved the lowest delamination factor under almost all cutting conditions, whereas the tool coating seemed to not really affect the delamination damage. This result can be attributed to the absence of tool wear in the drilling conditions used in this study. The TiAl/TiAlSiMoCr-coated tool achieved lower delamination damage at low and medium cutting speeds and under all feed rate conditions, while the hole quality was improved by increasing cutting speeds when drilling using the uncoated tool.

3.2.2. Morphologies and Geometries

For the same reasons that the choice of tool material and tool coating plays a part in meeting the stringent requirements of the aerospace industry for drilled-hole quality when drilling CFRP/Al stacks or FML composites, the selection of an appropriate drill bit geometry also represents a challenging but strategic step towards the success of the drilling process since it greatly impacts hole surface quality, delamination and tool performance. A wide range of cutting tool morphologies is available to carry out drilling operations, depending on the targeted materials and applications. Figure 13 exhibits the main morphologies of drills for which the drilling performance has been evaluated for various hybrid composite stack configurations [48,88,92,94,117,125,134,166]. Nevertheless, the conventional twist drill remains the tool commonly used by researchers [7,49,77,78,83,90,95,98–101,104,105,108,127–129,137,167–171], as it still represents the standard for industrial applications. Hence, it is required to optimize the main geometrical characteristics of this type of tool morphology to promote high-quality drilling of multi-material stacks. The geometry of the conventional twist drill is shown in Figure 14. It is mainly depicted by several angles—namely, the point angle, helix (or axial rake) angle, chisel angle and lip relief (or clearance) angle—and the number of flutes. These angles influence the amounts of cutting forces (thrust force and torque components), chip formation and thus delamination damage.

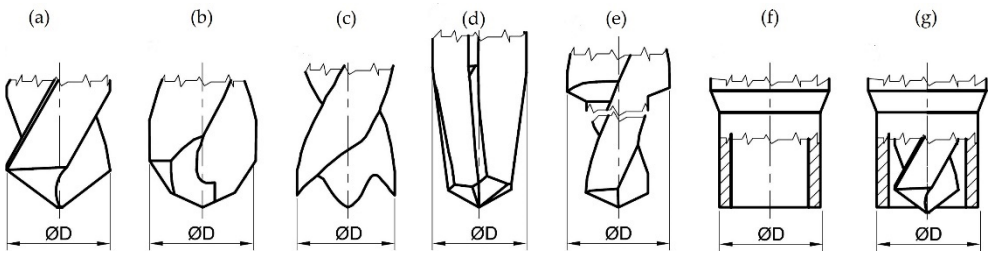

Figure 13. Morphologies of drill bits: (**a**) conventional twist drill, (**b**) double point angle (or double cone) twist drill, (**c**) brad and spur drill, (**d**) dagger drill, (**e**) step drill, (**f**) core drill and (**g**) special core drill [173].

Brinksmeier and Janssen [48] focused on the effect of tool morphology (conventional twist and step drills) on the deviation of the drilled-hole diameter when drilling CFRP/AlCuMg2 stacks (20/10 mm thick) at two different cutting speeds (10 and 20 m/min) and a feed rate of 0.15 mm/rev in dry conditions. The step drill was designed with a first step diameter of 15.4 mm and a second step diameter of 16.0 mm, which corresponds to the diameter of the conventional twist drill used in this study. Both drills were uncoated carbide tools with three flutes, a 30° helix angle and a 130° point angle. The authors explained that the step drill induced a better distribution of the mechanical load on the cutting edges and thus significantly improved the diameter deviations compared with those measured after drilling using the twist drill. Zitoune et al. [92] investigated the impact of the double

cone morphology on thrust force and hole quality when drilling T700-M21/AA2024 stacks (4.2/3.0 mm thick) at two spindle speeds (2020 and 2750 rpm) and three feed rates (0.05, 0.10 and 0.15 mm/rev) using 6.35 mm diameter uncoated tungsten carbide double cone drills with a 32.5° helix angle and three different L1/L2 ratios (0.33, 1.00 and 3.10). Figure 15 illustrates the principal lip length L1 and the secondary lip length L2 associated with the first point angle (132°) and second point angle (90°), respectively. They found that the double cone drill reduced the thrust force in comparison with the conventional twist drill due to the reduction in the theoretical average chip thickness caused by the addition of the secondary 90° point angle. However, they also reported that the double cone drills reduced the CFRP hole surface roughness in comparison with the conventional twist drill, since this type of tool morphology favored the occurrence of non-fragmented chips during the drilling of aluminum, which scratch the hole wall surface when they move along the cutting tool. Zitoune et al. [94] completed this experimental study with an ANOVA analysis and reported that L1/L2 ratios had little influence on thrust force (contributions in Al and CFRP were 2 and 9%, respectively), while the feed rate was the main contributing factor for both materials.

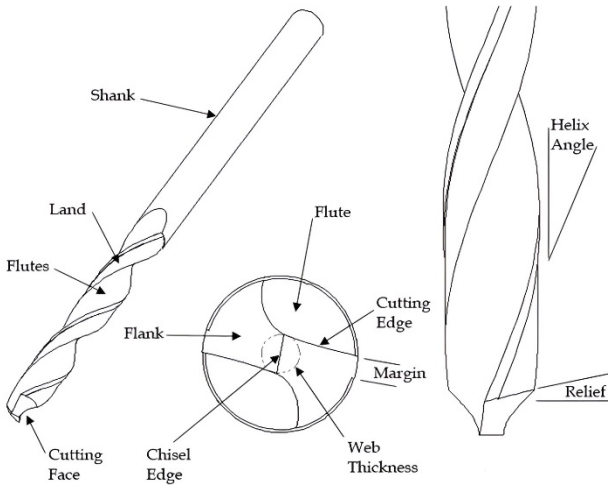

Figure 14. Geometry of conventional twist drill [174].

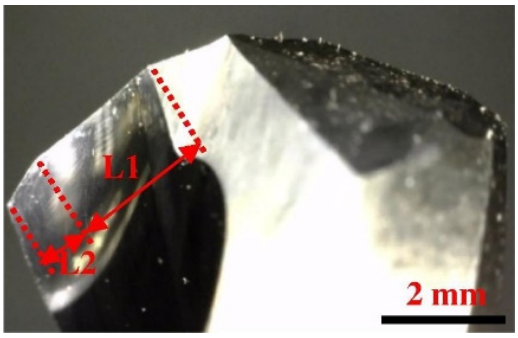

Figure 15. Definition of the principal and secondary lip lengths of the double cone drill [94].

Soo et al. [125] studied the impact of the double cone morphology on thrust force and hole quality when drilling CFRP/AA7010-T451 stacks (10.0/6.5 mm thick) at two cutting speeds (60 and 120 m/min) and two feed rates (0.15 and 0.30 mm/rev) using 6.38 mm diameter diamond-coated tungsten carbide drills with a 30° helix angle. The tools used in this study had double point angles (130/60° (double cone drill) and 140/180° (flat point drill)). The double cone drill was found to be unsuitable for drilling CFRP/AA7010-T451 stacks in dry conditions with the cutting parameters chosen for this study. This was attributed to the poor evacuation of long and non-fragmented metal chips and subsequent material adhesion, which caused the premature failure of the drill. The authors reported

that a flat point drill produced holes with good diameter accuracy. Moreover, the metal exit burr was found to be uniform around the circumference of the hole, with similar width and height (from 60 to 120 µm), which increased with the feed rate. Zhang et al. [88] researched the impact of brad and spur-like morphology on cutting forces, roughness and hole accuracy when drilling CCF300/AA7075-T7 stacks (3.07/3.10 mm thick) at various spindle speeds (2700, 3500, 4300, 5100 and 5900 rpm) and feed rates (0.03, 0.04, 0.05, 0.06 and 0.07 mm/rev) using 5 mm diameter diamond-coated cemented carbide drills in dry conditions. The brad and spur-like cutting tool exhibited two major cutting edges and a shorter chisel edge. The authors indicated that tool morphology contributed more significantly to the overall drilling performance than cutting parameters and concluded that the brad and spur-like drill promoted better results. They showed that hole accuracy was improved, since the average diameter deviation from nominal value ranged from 14 µm for the twist drill to 5 µm for the brad and spur-like drill. The authors attributed this positive result to the better self-centering capability of this tool morphology as well as the shorter chisel edge contributing more efficiently to the reduction in cutting resistance and the expansion of the heat dissipation area. The brad and spur-like drill also reduced thrust forces and provided better surface roughness in the CFRP layer. Indeed, the conventional twist drill produced CFRP holes with a surface roughness ranging from 2 to 4 µm, while the hole wall surface roughness achieved by the brad and spur-like drill varied between 1 and 2 µm. El Bouami et al. [134,166] investigated the influence of tool morphology (twist, step and brad and spur drills) on thrust force and hole quality when drilling T800H/AA2198 stacks (6.35/6.35 mm) at a cutting speed of 79 m/min and two feed rates (0.05 and 0.10 mm/rev) in dry conditions. The step drill was designed with a first step diameter of 4.7 mm and a second step diameter of 6.3 mm, which corresponds to the nominal diameter of the other drills used in this study. A value of 120° was chosen for the point angle of twist and step drills, and 56° was selected for the brad and spur drill. All of the drills were uncoated carbide tools with a 30° helix angle. The authors reported that both step and brad and spur drills reduced thrust force in both CFRP and AA2198 layers compared to the conventional twist drill, while the brad and spur drill caused little damage to the entrance hole perimeter. These results can be attributed to the ability of the step drill to lower thrust forces by cutting less material, whereas the two extreme points of the brad and spur drill facilitate the cutting of carbon fibers and thus delay the delamination occurrence. El Bouami et al. [166] also performed an ANOVA analysis to assess the effect of cutting speed (59, 79 and 99 m/min), feed rate (0.05, 0.075 and 0.100 mm/rev) and point angle (120, 130 and 150°) on thrust force and delamination. Both the point angle and feed rate were found to be the predominant factors (44.66 and 33.09%, respectively) on thrust forces in the CFRP panel, while only the point angle had a significant influence (76.06%) on thrust force in the aluminum panel. This investigation also showed that the drilling of CFRP/aluminum stacks required sufficiently high feed rates to produce fragmented chips and to thus obtain better hole quality in the aluminum layer. However, a higher feed rate also caused a reduction in CFRP hole quality. In addition, the authors reported that the interaction between cutting speed and feed rate contributed (14.43%) to the severity of the CFRP damage, but the point angle was the main contributing factor (45.63%) affecting delamination, and a lower point angle produced less delamination damage due to the better shearing of fibers. Benezech et al. [131] studied the influence of the axial rake angle (0, 10, 20, 30 and 40°) and point angle (120, 135 and 150°) on aluminum chip morphology and thrust force in CFRP when separately drilling the aluminum and composite constituents of T800-M21/AA2024 (10/10 mm thick) stacks. Drilling experiments were carried out using 8 mm diameter uncoated twist drills at a spindle speed of 6000 rpm and various feed rates (0.02, 0.04, 0.06 and 0.08 mm/rev). They highlighted the relationship between the rake/point angle couple and AA2024 chip morphology and concluded that a rake angle of 30° achieved short and fragmented chips for any point angle value. Moreover, the authors found that both rake and point angles influenced the magnitude of thrust force when drilling the T800-M21 component. For the studied range of point angles, thrust force decreased with increasing rake angle. A drop in

thrust force was also observed with increasing point angle, which is consistent with the trend found by El Bouami et al. [166]. However, the magnitude of this drop turned out to be less significant for a rake angle higher than 30°.

Hassan et al. [95] focused on the effect of the helix angle (15 and 30°), clearance angle (6 and 8°), point angle (110 and 130°) and chisel edge angle (30 and 45°) on the difference between the hole diameters of CFRP and aluminum, hole surface roughness and aluminum burr height when drilling CFRP/AA7075-T7 stacks (3.587/3.317 mm thick) using 4.826 mm diameter uncoated tungsten carbide twist drill bits at two spindle speeds (1500 and 2600 rpm) and two feed rates (0.05 and 0.10 mm/rev) in dry conditions. They found that the diameter difference was reduced when increasing the clearance or helix angles as well as when decreasing the point or chisel edge angles. The hole surface roughness of both CFRP and AA7075-T7 holes was made smoother by decreasing the helix and chisel edge angles. The clearance and point angles had different impacts on the hole surface roughness depending on the material being drilled. Thus, increasing the clearance angle resulted in an improvement in the surface roughness of CFRP holes and the deterioration in that of AA7075-T7 holes, while increasing the point angle only improved the surface roughness of AA7075-T7 holes without modifying that of the CFRP holes. The metal burr height was found to be lower when decreasing the helix, clearance or chisel edge angles or when increasing the point angle. Finally, the authors concluded that the best hole quality of CFRP/Al stacks, which was characterized by the achievement of the minimum difference in diameter, minimum hole surface roughness and minimum burr height formation, could be achieved with a spindle speed of 2600 rpm and a feed rate of 0.1 mm/rev using a drill bit with an optimal combination of a helix angle of 15°, a primary clearance angle of 8°, a point angle of 130° and a chisel edge angle of 30°. Hassan et al. [77] further studied in more detail the effect of the clearance angle (6, 7 and 8°), point angle (130, 135 and 140°) and chisel edge angle (30, 37.5 and 45°) on the maximum thrust force and hole surface roughness. Drilling tests were performed on CFRP/AA7075-T6 stacks (3.587/3.317 mm thick) using 4.826 mm diameter uncoated tungsten carbide twist drill bits at a spindle speed of 2600 rpm and a feed rate of 0.05 mm/rev in dry conditions. ANOVA and RSM were established to determine the explicit impact of drill geometry parameters and their interactions on drilling performance. The authors found that the lowest thrust force for the CFRP layer was produced with a tool geometry with an 8° clearance angle, 140° point angle and 30° chisel edge angle, while the lowest thrust force for the AA7075-T6 layer was generated with a tool geometry with a 7° clearance angle, 130° point angle and 37.5° chisel edge angle. The clearance angle was found to significantly affect the maximum thrust force for both materials (58.78 and 52.34%, respectively), while the point angle had an insignificant effect (1.71 and 0.95%, respectively). Moreover, the maximum thrust force for both CFRP and AA7075-T6 was smaller when decreasing the clearance and chisel edge angles. They also reported that the lowest CFRP hole surface roughness was achieved with a tool geometry with a 6° clearance angle, 140° point angle and 45° chisel edge angle, while the lowest AA7075-T6 hole surface roughness was generated with a tool geometry with a 6° clearance angle, 130° point angle and 45° chisel edge angle. For CFRP holes, the primary angle contributed greatly to surface roughness, followed by the clearance angle–point angle interaction and point angle (35.07, 20.97 and 10.92%, respectively), while AA7075-T6 hole surface roughness was affected by the point and clearance angles (53.92 and 22.15%, respectively). In addition, increasing the chisel edge angle or decreasing the clearance angle promoted smoother surface roughness for both materials. The authors attributed these results to the fact that a higher chisel edge led to a greater shear angle, which contributed to lower chip thickness, while the worst cutting conditions were obtained at a higher clearance angle, which favored the chipping of the cutting edge and thus caused an obstruction in the drilled hole. Finally, the authors used a multi-objective optimization method, and the combination of a 45° chisel edge angle, 7° primary clearance angle and 130° point angle was found to be the optimal drill geometry that would be able to achieve minimum thrust force and the best hole surface roughness when drilling CFRP/AA7075-T6 stacks in a

single-shot process. Bayraktar and Turgut [168] performed ANOVA and RSM in order to identify the impact of cutting speed (100, 125 and 150 m/min), feed rate (0.1, 0.2 and 0.3 mm/rev) and point angle (90, 118 and 135°) on delamination occurrence in entrance and exit holes when drilling CFRP/A6013-T651 stacks using 8 mm diameter uncoated and TiN- and TiAlN-coated HSS drills with a 30° helix angle. The most effective parameter on the hole entrance and exit delamination of the CFRP constituent was determined to be the feed rate, followed by the drill point angle and cutting speed, respectively. A reduction in delamination formation was observed when decreasing the point angle due to the reduction in thrust force with the point angle. The authors reported that the uncoated cutting tool produced less delamination than TiN- and TiAlN-coated drill bits, and the entrance and exit delamination factors were similar for both of these coated tools. This result can be attributed to the reduction in the sharpness of the cutting edge caused by the deposition of coating, which creates more difficulties for the cutting tool to penetrate the material.

The impact of tool morphology on thrust force, hole diameter and burr size during FML drilling has been discussed by a few authors [117,169]. Pawar et al. [169] carried out drilling experiments on GLARE 5 and GLARE 6 specimens with 6.35 mm diameter uncoated solid carbide twist drill bits with a helix angle of 30°, point angle of 120° and four different drill point geometries (i.e., two-fluted, three-fluted, four-faceted and eight-faceted drills), as shown in Figure 16. Three spindle speeds (4500, 6000 and 7500 rpm) and feed rates (0.150, 0.225 and 0.300 mm/rev) were tested. The authors found that the lowest thrust force and torque were provided by the two-fluted tool, closely followed by the four-faceted drill (with a gap of 20 N), regardless of the cutting parameters. These point geometries also achieved holes with diameters closer to the nominal one compared with the other tools. The worst thrust force was obtained with the three-fluted drill, while the eight-faceted drill generated the worst torque. Adhered aluminum at the cutting edge and drill point were observed for these two cutting tools. Furthermore, the holes made in the FML with all of the tools were undersized, but the undersize was found to be the maximum with the eight-faceted drill due to the uncut fibers left after drilling. At the exit hole, the authors observed that the eight-faceted tool gave rise only to uniform metal burrs without caps, with the greatest height (up to 2 mm) and width (up to 160 µm). The authors attributed this result to the clogging of the flute by chips caused by lower clearance, resulting in heating during the drilling process, thus promoting plastic deformations of aluminum. Otherwise, the three other drill point geometries produced uniform burrs with and without caps, and the maximum values of height and width were much lower (150–400 µm and 65–70 µm, respectively) relative to those achieved using the eight-faceted drill.

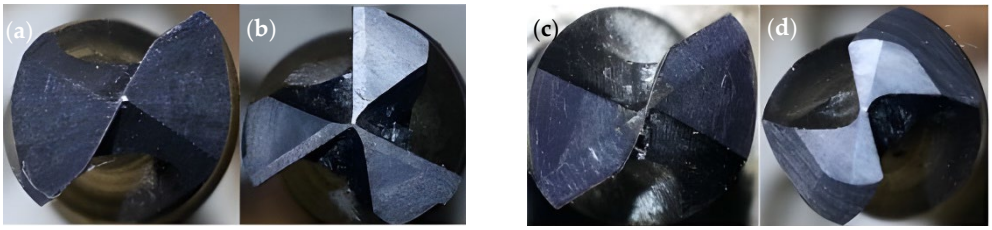

Figure 16. Drill point geometry: (**a**) 2-fluted, (**b**) 3-fluted, (**c**) 4-faceted and (**d**) 8-faceted [169].

Rezende et al. [117] also investigated the impact of tool morphology (two-fluted and three-fluted twist drills and a brad and spur drill) on thrust force and burr height when drilling Al/PE/Al sandwich composite (4 mm total thickness) using 5 mm diameter uncoated tungsten carbide drills at three cutting speeds (24, 48 and 72 m/min) and three feed rates (0.05, 0.10 and 0.15 mm/rev) in dry conditions. The authors found that the evolution of thrust force differed during the cutting of each layer, depending on tool morphology. Indeed, the lowest thrust force was provided by the brad and spur tool during the drilling of Al layers, while the twist drills performed the best in terms of thrust force when drilling the composite part. Moreover, an ANOVA analysis of the results was performed, and the authors found that tool morphology and cutting speed were the

prominent factors influencing thrust force, while tool morphology and feed rate were the main contributing factors for burr height.

3.2.3. Tool Wear

Tool wear represents another challenging issue when drilling CFRP/Al stacks or FML composites. Although the selection of cutting parameters and tool geometry is performed in order to ensure the industrial requirements for drilled-hole quality of multi-material stacks, it is also essential to focus on tool wear since this phenomenon directly affects the drilling performance, can shorten tool life drastically and hence increase the manufacturing costs. Several authors [7,49,88,90,96,104,125,134] investigated tool wear and its impact on tool performance when drilling hybrid composite stacks by evaluating the evolution of thrust force, surface roughness or hole diameter as a function of the number of drilled holes before the total wear of the tool. Nevertheless, no article reporting the consequences of tool wear on the drilling performance for FML materials can be found in the scientific literature.

Zitoune et al. [7] studied the effect of tool wear on cutting forces (thrust force and torque components) when drilling T700-M21/AA2024 stacks (4.2/3.0 mm thick) at a spindle speed of 2020 rpm and a feed rate of 0.1 mm/rev using a 6 mm diameter uncoated tungsten carbide drill bit. They found that CFRP cutting forces increased steadily up to 30 holes and achieved a stable magnitude from 30 to 60 holes, corresponding to the normal wear region. Furthermore, Zitoune et al. [90] showed that the rise in CFRP thrust force with the number of drilled holes was less when drilling with nano-coated tools of the same CFRP/Al stack than in the previous study [7]. This can be attributed to the lower wear of the coated tool. Montoya et al. [49] reported similar results when drilling CFRP/AA7010-T7451 stacks (7/14 mm thick) at a spindle speed of 3000 rpm and a feed rate of 0.04 mm/rev using 6 mm diameter uncoated and coated (diamond/TiAlCrN/AlTiSiN-G) tungsten carbide drills with a 124° point angle and a 30° helix angle. The average thrust force generated by the diamond-coated tool gradually increased with the number of holes, with more moderate results than with the uncoated tool. In addition, the authors reported that the evolution of the diameter difference between CFRP and AA7010-T7451 holes was stable for both uncoated and diamond-coated tools and not influenced by the deposition of diamond coating. The surface roughness of the holes drilled using the uncoated tool increased significantly with the number of holes until it exceeded the acceptable roughness in the aeronautics industry (3.2 µm R_a in CFRP) at the 75th hole. In contrast, the diamond coating reduced tool wear and thus achieved the best surface roughness (about 0.2 µm *Ra* in Al and 1.2 µm R_a in CFRP) after 250 drilled holes, without a large fluctuation depending on the number of holes. Zhang et al. [88] also examined the influence of tool wear on thrust force and hole quality when drilling CCF300/AA7075-T7 stacks (3.07/3.10 mm thick) at a spindle speed of 4000 rpm and a feed rate of 0.04 mm/rev using two different geometries of a 5 mm diameter diamond-coated cemented carbide twist drill bit in dry conditions. The thrust forces of both CFRP and AA7075-T7 constituents were found to increase steadily up to 400 holes and then rise sharply due to the loss of sharpness of the cutting edge caused by the rapid wear of the drill bit. It was also noted that the flank wear V_B suddenly deteriorated, and the hole quality declined dramatically, with surface erosion or tearing within the CFRP hole and large burrs at the aluminum exit hole. D'Orazio et al. [104] highlighted the correlation between tool wear mechanisms and thrust force, hole diameter and delamination when drilling CFRP/AA7075-T651/CFRP stacks (2.8/20.0/2.8 mm thick) using two different 6.8 mm diameter twist drills, including DLC- and nanocomposite TiAlN-coated tools. Drilling experiments were performed in wet conditions, with a chip removal cycle consisting of two passes, using a reverse motion required to remove chips. The authors reported that the flank wear, peak thrust force and delamination factor increased with the number of drilled holes, irrespective of the chosen coating, while the hole diameter in both CFRP and AA7075-T651 layers decreased. Furthermore, it was found that the evolutions of thrust force, delamination factor and hole diameter were not affected by the choice of coating, while the rise in flank wear of the TiAl-coated tool with the number

of drilled holes was stressed compared to the progression of flank wear observed on the DLC-coated tool. The authors used third-degree polynomial regression models to correlate flank wear and peak thrust force and delamination, as well as the peak thrust force in the CFRP layer and the delamination factor. Hence, they concluded that the increase in the delamination factor and thrust force and the decrease in the hole diameter with increasing flank wear confirmed that the rise in the delamination factor with the number of holes was strongly dependent on tool flank wear. They also confirmed that the delamination factor depended on thrust force. Kuo et al. [103] carried out drilling tests on CFRP/AA7075-T6 stacks (3.5/3.0 mm thick) using a vibration-assisted drilling process and studied the impact of the number of drilled holes on flank wear and metal burr height. The tool life of 6.375 mm diameter diamond-coated double cone drills with a 40° helix angle and an L1/L2 ratio (the principal lip length L1 and the secondary lip length L2 were associated with the first point angle (120°) and second point angle (20°), respectively) of 1.74 was tested at different cutting speeds depending on the drilled material (CFRP: 130, 150 and 170 m/min; AA7075-T6: 200 m/min), feed rates (0.04, 0.06 and 0.08 mm/rev), low vibration frequencies (45, 50 and 55 Hz) and high amplitudes (5, 20 and 50 μm). For all of the tested drilling parameters, it was found that flank wear, which was greater on L1 than on L2, increased gradually with the number of drilled holes. The lowest flank wear after drilling 200 holes (L1: 29.8 μm; L2: 37.7 μm) was recorded when relatively low thrust forces occurred, at a vibration frequency of 50 Hz, the lowest amplitude and the highest cutting speed and feed rate. The greatest flank wear at the last hole (L1: 59.6 μm; L2: 74.7 μm) was observed when high thrust forces were generated, at the lowest cutting speed and at the highest feed rate, frequency and amplitude. The authors performed an ANOVA analysis to highlight the factors impacting the flank wear on the principal and secondary cutting edges of the cutting lip. They reported that the amplitude was the greatest contributing factor affecting the flank wear on L1 (43.14%), followed by cutting speed (34.39%) and frequency (16.40%), while only cutting speed and amplitude influenced the flank wear on L2 (55.83 and 27.61%, respectively). Hence, lower flank wear could be achieved by increasing cutting speed or decreasing the frequency and amplitude. Moreover, increasing the number of drilled holes, and thus tool wear, seemed to significantly increase burr height only at the highest feed rate (0.08 mm/rev), while it was less visible at other feed rates. The highest burrs (~0.2 mm) were observed at the lowest feed rate (0.04 mm/rev), while the lowest ones (~0.02 mm) were recorded at the highest feed rate, regardless of the chosen values for the other cutting parameters. The ANOVA analysis of the results confirmed that burr height was mostly impacted by feed rate (96.02%), and its minimization could be obtained by increasing the feed rate; this is consistent with the results found in [95,99,117,128,171]. Soo et al. [125] investigated the influence of the number of drilled holes on flank wear, cutting forces, hole diameter, metal burr size and delamination when drilling CFRP/AA7010-T451 stacks (10.0/6.5 mm thick) at two cutting speeds (60 and 120 m/min) and two feed rates (0.15 and 0.30 mm/rev) using 6.38 mm diameter diamond-coated tungsten carbide flat point drills with a 30° helix angle. They found that flank wear increased progressively with the number of drilled holes and did not exceed 40 μm after 120 holes; this is consistent with the findings of Kuo et al. [103]. They noted that lower flank wear was obtained at a lower feed rate, regardless of the cutting speed. Cutting forces were found to be relatively stable when increasing the number of drilled holes; this is probably due to the low level of wear observed on the drills. In all cases, the diameters of the holes drilled in both materials were oversized, and their values seemed to decrease slightly when increasing the number of drilled holes. An improvement in the deviation from the nominal diameter was nevertheless observed at the highest feed rate. The authors also reported that the impact of the number of drilled holes on exit burr height and delamination was not the same, depending on the feed rate. Thus, more delamination damage and smaller burrs were produced when increasing the number of drilled holes at a higher feed rate, whereas the exit burr width was generally larger in all drilling conditions when the number of drilled holes increased. However, the impact of tool wear on delamination damage was negligible since the variation in

the delamination factor was very small. Fernández-Vidal et al. [124] investigated the impact of the wear on the drilling performance of 7.92 mm diameter uncoated double cone drills (140/118°) with a 29.82° helix angle when drilling T800S-M21/AA7075-T6 stacks (4.50/4.86 mm thick) at a cutting speed of 145 m/min and a feed speed of 250 mm/min in dry conditions. In agreement with previous results [7,49,88,104], they found that the thrust forces for both materials increased with the number of drilled holes. The fact that the thrust force generated for AA7075-T6 increased significantly depending on the number of drilled holes when drilling the multi-material stack, while it remained constant when drilling only the aluminum part, was also noted. The evolution and magnitude of thrust force recorded for the CFRP layer when drilling a multi-material stack were similar to those for the CFRP part drilled separately. The authors reported that the diameter of the CFRP hole increased slightly when increasing the number of drilled holes for CFRP/Al stacks, while its value decreased when only the CFRP part was drilled. Furthermore, smaller diameter differences between T800S-M21 CFRP and AA7075-T6 holes were found when drilling both materials together compared to those produced separately, regardless of the number of drilled holes. Banon et al. [96] evaluated the hole diameter and hole surface roughness depending on the number of drilled holes when drilling CFRP/AA2024 stacks (2/8 mm thick) with the same cutting tool as that used by Fernández-Vidal et al. [124]. Experiments were carried out in dry conditions at three cutting speeds (85, 115 and 145 m/min) and three feed speeds (200, 250 and 300 mm/min). The authors showed that the hole wall surface roughness of both materials decreased as the number of drilled holes increased due to both abrasive and adhesive wear of the tool. After drilling 20 holes, the lowest roughness in both materials (R_a of 2.67 and 2.58 µm for CFRP and AA2024, respectively) was found at the highest cutting speed and the lowest feed speed, while the highest roughness in both materials (R_a of 7.47 and 12.22 µm for CFRP and AA2024, respectively) was measured with the lowest cutting and feed speeds. Contrary to surface roughness, the authors stated that the diameters evaluated in both materials did not seem to be affected by the number of drilled holes, although it was shown that the increase in cutting speed generated less dispersion.

3.3. Selection of Cutting Process

The selection of appropriate cutting parameters and optimized tool geometries alone is not enough to sufficiently improve the drilling performance of aerospace assemblies, reduce drilling-induced delamination, extend tool life and thus limit manufacturing costs associated with the drilling of hybrid composite stacks and FML composites. High-performance cooling strategies, such as minimum quantity lubrication (MQL) or cryogenic cooling, as well as unconventional drilling methods, including vibration-assisted drilling (VAD) and orbital drilling (OD), represent an inevitable alternative and answers to the aforementioned issues regarding the single-shot drilling of CFRP/Al stacks and FML composites.

3.3.1. Alternative Methods

Vibration-assisted drilling consists of superposing an axial sinusoidal oscillating motion of the drill in the axial feed direction during the drilling process using a mechanical or piezoelectric oscillator, as illustrated in Figure 17. The intermittent disengagement of the drill bit from the material induces a significant reduction in thrust force and cutting temperature, as well as easier chip fragmentation and evacuation, which may result in delamination-free holes and tool life enhancement when drilling composite laminates. VAD is controlled by two parameters, frequency and amplitude. Low-frequency, high-frequency and ultrasonic vibration-assisted drilling, abbreviated LF-VAD, HF-VAD and UAD, respectively, are distinguished based on the range of frequencies selected for drilling. LF-VAD is performed at frequencies lower than 1 kHz, while HF-VAD is associated with frequencies ranging from 1 kHz to 20 kHz. VAD with frequencies higher than 20 kHz is qualified as ultrasonic (UAD). The choice of vibration amplitude, coupled with an appropriate selection of vibration frequency and cutting conditions, determines the ability of the VAD process to easily fragment chips. Several studies on the overall drilling performance of the VAD tech-

nique were carried out for CFRP [175–179], for CFRP/Ti stacks [110,147,149,150,180–192] and, more recently, for CFRP/Al stacks [103,109,110].

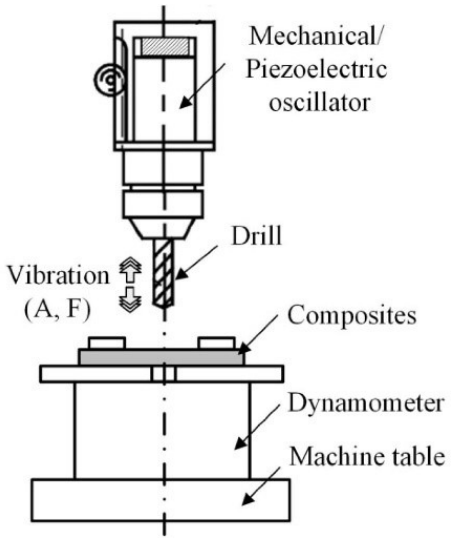

Figure 17. Illustration of vibration-assisted drilling [31].

Kuo et al. [103] studied the influence of cutting speed (CFRP: 130, 150 and 170 m/min; AA7075-T6: 200 m/min), feed rate (0.04, 0.06 and 0.08 mm/rev), vibration frequency (45, 50 and 55 Hz) and amplitude (5, 20 and 50 μm) on the performance of a VAD process in terms of cutting force, flank wear, metal burr height and hole diameter for CFRP/AA7075-T6 stacks (3.5/3.0 mm thick). Drilling tests were performed in dry conditions using a 6.375 mm diameter diamond-coated double cone drill with a 40° helix angle and an L1/L2 ratio (the principal lip length L1 and the secondary lip length L2 were associated with the first point angle (120°) and second point angle (20°), respectively) of 1.74. The ANOVA analysis of the results showed that the vibration amplitude did not perturb the exit burr height, while it was the prominent contributing factor impacting the thrust force for both CFRP and AA7075-T6 layers (80.14 and 48.14%, respectively), as well as the flank wear on L1 (43.14%), the second most important factor after cutting speed regarding the flank wear on L2 (27.61%) and the third one after feed rate and frequency for the diameter in the CFRP layer (18.33%). Additionally, the influence of frequency was mostly negligible for almost all of the monitored outputs, although it noticeably impacted the hole diameter in the CFRP layer, the flank wear on L2 and the thrust force for the AA7075-T6 layer (37.22, 16.40 and 16.07%, respectively). The authors stated that it was suitable to select a lower amplitude in order to lessen thrust force and flank wear. The lowest flank wear was recorded, regardless of the number of drilled holes, when relatively low thrust forces occurred, at high vibration frequency, at the lowest amplitude and at the highest cutting speed and feed rate. This result was attributed to the intermittent contact between the tool and workpiece, reducing cutting time and friction-induced heat, thereby reducing tool flank wear. A detailed comparison of conventional and LF-VAD of CFRP/AA7175 (10.0/4.5 mm thick) using 6.35 mm diameter diamond-coated cemented carbide twist drills with a point angle of 118° was carried out by Seeholzer et al. [109] to evaluate the influence of cutting speed (60 and 90 m/min), feed rate (0.04 and 0.075 mm/rev) and vibration amplitude (6, 30, 60, 90 and 120 μm) on delamination at the CFRP entrance, burr height at the AA7175 exit, cutting forces, temperature and deviation from the nominal diameter in both materials. In this study, delamination was assessed using both the delamination factor F_d and the quality function Q_d defined by Voss et al. [193], which incorporated cracks, spalling, delamination and uncut fibers. The authors reported that LF-VAD produced more extensive delamination, accentuated by increasing vibration amplitude, compared to conventional drilling (CD). Moreover, LF-VAD generated smaller exit burrs than those obtained by CD, and their

height decreased when increasing the vibration amplitude, but only at a cutting speed of 90 m/min and a feed rate of 0.075 mm/rev. Hence, the lowest temperature was found at the highest cutting speed, feed rate and vibration amplitude values. However, LF-VAD was considered better than CD in order to minimize cutting forces and reduce cutting temperatures in both materials, more significantly at a high cutting speed and feed rate. The authors also reported that all of the drilled holes were oversized for both materials, and the hole diameter for the CFRP layer was always larger than that for the AA7175 layer, regardless of the drilling strategy. Nevertheless, the disturbing tool vibrations induced by the superimposed sinusoidal oscillation during the LF-VAD process caused larger diameter values than those generated by CD. Furthermore, the cutting conditions significantly impacted the deviation from the nominal diameter obtained by LF-VAD, contrary to CD. Indeed, higher amplitude-to-feed-rate ratios generally resulted in significant deviations from the nominal hole diameter. The impact of chip size on chip transport was analyzed by measuring the temperatures in the CFRP constituent with and without Al-chip transport. The resulting temperatures in CFRP were always higher than the maximum temperature in the aluminum layer and increased when the metal chip transport through the tool flute was considered for CD. The rise in temperature was higher when the speed rate was high; this was attributed to the higher probability of accumulating chips around the drill since the increase in the feed rate led to thicker chips. The authors reported that the maximum temperature in CFRP without Al-chip transport was significantly reduced, regardless of the cutting parameters, and the lowest temperature was found at the highest cutting speed, feed rate and vibration amplitude values, which were the same conditions allowing the minimization of the exit burr height. In addition, small and fragmented chips were observed when the LF-VAD process was performed at both a high vibration amplitude and a high feed rate, while continuous and ribbon-shaped chips were always generated by CD for the overall tested cutting parameters. The difference between the temperatures in CFRP with and without Al-chip transport increased. This phenomenon was attributed to the superposition of a longer drilling duration with longer chip/workpiece interaction. Zou et al. [110] investigated the feasibility of improving the hole size accuracy and reduce defects observed at the periphery of the drilled hole when drilling a co-cured specimen composed of 10 mm thick aluminum AA7050 between two 5 mm thick T700 CFRPs by LF-VAD. The experiments were performed in dry conditions with a 6.36 mm diameter uncoated tool with a point angle of 140°, at a frequency of 25 Hz and at various spindle speeds (1000, 1500, 2000, 3000 and 4000 rpm), feed rates (0.02, 0.03 and 0.04 mm/rev) and vibration amplitudes (0, 10, 20, 30, 40 and 50 µm). The influence of these parameters on cutting force, cutting temperature, chip formation, hole quality and hole topography was analyzed, and the drilling performance of LF-VAD was compared to that of CD. The results showed that LF-VAD contributed significantly to the reduction in average thrust forces in both materials and in maximum drilling temperatures, which was caused by the beneficial chip breaking effect induced by this unconventional drilling process, while an increase in the maximum thrust forces was observed in both materials when the vibration amplitude rose. For both CD and LF-VAD processes, the authors also noticed that a lower feed rate and higher spindle speed promoted smaller mean thrust force during CFRP AA7050 phases, while a higher feed rate and lower spindle speed must be used to minimize the maximum drilling temperature. Nevertheless, the beneficial impact of the increase in vibration amplitude on cutting temperature was valid only up to 30 µm, because after this value, the heat induced by the increase in the maximum thrust force with the elevation of vibration amplitude became more significant and inevitably led to a slight rise in the maximum temperature. Moreover, an improvement in both cylindricity and deviation between the drilled-hole size and nominal diameter of the drill bit, especially for the upper CFRP layer, was observed when increasing the vibration amplitude. It was also demonstrated that LF-VAD could greatly improve the surface quality of the lower interface, even more so when the vibration amplitude was high, owing to the reduction in the thermal effect, while the CFRP hole wall

surface defects, such as grooves or surface cavities, induced by a high thermal effect, were significantly reduced by the LF-VAD process due to the lower cutting heat.

Orbital drilling, also named helical milling, produces holes using an end mill that rotates around its own axis while being driven by a helical advance, as depicted in Figure 18. Thus, the diameter of the drilled hole depends on both the tool, whose diameter is lower than the nominal diameter of the hole, and the helical path diameter. According to Wang et al. [194], the combination of a limited contact region between the tool and workpiece and sufficient removal space results in lower cutting forces and temperature and promotes higher hole quality. Indeed, there is a radial clearance between the cutting tool and the drilled hole due to the deviation of the end mill diameter from the nominal diameter of the drilled hole, which favors chip evacuation from the cutting area. Chip evacuation is also facilitated by the discontinuous cut, which fragments chips during the OD process and thus eliminates the recurring chip jamming issues commonly observed during CD [195]. Therefore, efficient chip evacuation prevents the temperature from rising and thus reduces the occurrence of both matrix burn in composite laminates and regions affected by heat in metals. Very few investigations on the ability of the OD process to achieve high-quality drilled holes have been performed for CFRP [196–199], CFRP/Ti [43,194,195,200–203] and CFRP/Al stacks [102,136].

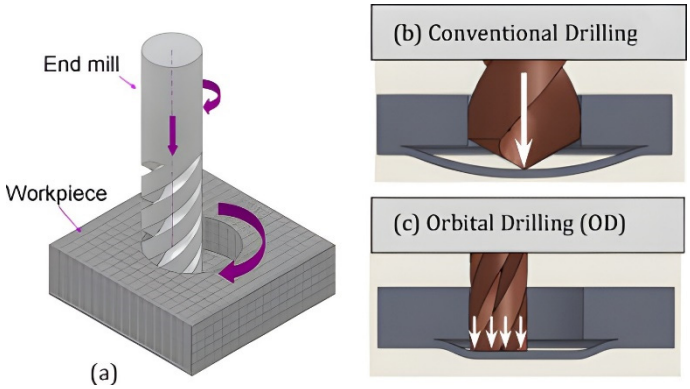

Figure 18. (**a**) Illustration of orbital drilling; deflection of the last ply in (**b**) CD and (**c**) OD [196].

Wang et al. [136] proposed to evaluate the hole quality of CFRP/AA2024-T3 stacks (6/6 mm thick) drilled by the OD process using an 8 mm diameter solid nano-copper-coated carbide three-fluted milling tool with a 45° helix angle, 20° clearance angle and 9° rake angle. A two-step strategy was employed to reduce push-down delamination. It consisted of drilling, from CFRP to AA2024-T3, the first hole with a diameter smaller than the required diameter. Then, the second hole was drilled with the target diameter by reversing the stacking sequence. The results from this drilling process were compared to those obtained by CD using two different diameters of TiAlN-coated solid carbide twist drills with a 140° point angle and 30° helix angle. The first step was performed with a diameter of 8 mm, while the second step was carried out with a diameter of 10 mm. The influence of spindle speed (1000, 2000 and 3000 rpm) and feed speed (5, 10 and 15 mm/min) on thrust force and the delamination factor was also analyzed for both drilling processes. It was found that hole drilling by OD significantly reduced thrust force compared to that of CD and led to the elimination of defects, such as uncut fibers or fiber pull-out, observed at the entry and multi-material interface. Furthermore, the increase in spindle speed when holes were drilled by OD caused a more significant reduction in thrust force than that observed when CD was used. Hence, it was recommended to perform OD at higher spindle speeds and lower feed speeds to reduce thrust force and thus promote delamination-free holes. Bolar et al. [102] also compared the performance of CD and OD processes in terms of cutting forces, chip morphology, cutting temperature, surface roughness, hole accuracy and burr size for hole-making in CARALL composed of carbon fiber prepreg

and AA2024 aluminum layers stacked alternately. Drilling tests were carried out using a 6.8 mm diameter solid carbide two-fluted twist drill with a 140° point angle at three cutting speeds (45, 65 and 85 m/min) and two feed rates (0.02 and 0.04 mm/rev), while helical milling experiments were performed using a 5 mm diameter carbide two-fluted end mill at the same cutting speeds as those used for CD, two axial feeds (0.2 and 0.4 mm/rev) and a tangential feed of 0.1 mm/tooth. As found by Wang et al. [136] for CFRP/AA2024-T3 stacks, the OD process also exhibited lower thrust force than that measured during CD, and higher spindle speeds and lower feed speeds were recommended to reduce the thrust force generated on CARALL. Chip formation and cutting temperature are known to determine the roughness of the drilled holes. The authors reported that the cutting temperatures measured during the OD process were drastically reduced compared to those monitored during CD, irrespective of the cutting conditions, due to intermittent cutting, which favored chip evacuation and heat dissipation. The lowest cutting temperature was achieved at the lowest cutting speed and axial feed. In addition, long and non-fragmented chips were generated during CD, while OD produced short and fragmented chips, which promoted smoother hole surface roughness. However, the size of the chips, measured as exit burr size, was found to be related to axial feed and, to a lesser extent, to cutting speed, and the authors warned that excessive axial feed could result in tool deformation and chatter, leading to surface quality deterioration. The best surface roughness was generated at the highest cutting speed and axial feed. In addition, the two hole-making processes produced oversized entrance and exit holes, but the OD process allowed a clear reduction in the deviation from the nominal diameter due to smaller and fragmented chips compared to those produced by CD and achieved the required H9 diameter tolerance. The best results were found at the lowest cutting speed and axial feed. The authors reported that smaller and thinner exit burrs were generated when decreasing both cutting speed and feed rate, regardless of the hole-making process. Hence, exit burr size was minimized at the lowest cutting speed and axial feed.

3.3.2. Cooling Strategies

Although the use of cutting fluids can enhance the machining efficiency and improve the tool life by dissipating the heat produced at the cutting region, the cyclic utilization of coolant in composite–metal stack drilling processes is uneconomical and environmentally unfriendly due to heavy pollution by powdery CFRP chips, justifying the interest in reducing its use [77]. However, it may be wise to pay particular attention to the cutting environment since the appropriate selection of the cooling conditions, minimizing the required amount of cutting fluid, could contribute to promoting high-performance drilling of hybrid composite stacks or FML composites. Hence, the development of alternative environmentally friendly cooling techniques that allow a reduction in friction between the cutting tool and the chip, limit the adhesion of metal to the cutting edge and lessen the cutting temperature is required to substitute conventional unhealthy and environmentally hazardous flood cooling methods while ensuring extended tool life and improved drilled-hole quality. Among the various existing cooling strategies, minimum quantity lubrication (MQL) and cryogenic cooling are the two main high-performance cooling techniques that have emerged concerning the drilling of multi-material stacks, although, to date, few authors have investigated the drilling performance of these two cooling techniques when drilling CFRP/Al stacks [4,48,49,93] and GLARE [107,204,205]. MQL consists of applying a fine mist to the cutting zone using the optimal amount of cutting fluid with compressed air. The performance of this new "green" cooling technique was already studied when drilling aluminum alloys [206–208], CFRP [209] and CFRP/Ti stacks [181,183,190,192,210,211]. Cryogenic cooling consists of projecting a super-cold medium, such as liquid nitrogen (LN_2) or liquid carbon dioxide (LCO_2), at high velocity to quickly dissipate the heat generated at the tool–workpiece interface. Some investigations of the efficiency of this alternative solution of dry machining were also carried out in the case of the drilling of CFRP panels [209,212–215] and CFRP/Ti stacks [216,217].

Brinksmeier and Janssen [48] compared the deviation of the drilled-hole diameters and tool wear achieved in MQL and dry conditions when drilling CFRP/AlCuMg2 stacks (20/10 mm thick) at two different cutting speeds (10 and 20 m/min) and a feed rate of 0.15 mm/rev using a 15.4/16.0 mm diameter uncoated carbide step drill with three flutes, a 30° helix angle and a 130° point angle. The authors reported that the penalizing effects of the cutting temperature on the hole diameter and tool wear were alleviated by using MQL since tighter diameter tolerances than those generated in dry conditions were achieved due to improved friction conditions, which facilitated chip removal. In addition, the progression of tool wear was delayed because the BUE occurrence at the cutting edge and the flank of the cutting tool was found to be clearly reduced after several drilled holes. Meshreki et al. [93] studied the effect of four different cooling modes (dry, MQL(LP-HF) with low pressure (<1.5 bar) and a high flow rate (400 mL/h); MQL(HP-LF) with high pressure (4.25 bar) and a low flow rate (10 mL/h) and flood cooling) on thrust force, cutting temperature, delamination, surface roughness and diameter errors when drilling CFRP/Al stacks (19/19 mm thick) at a cutting speed of 76 m/min and a feed rate of 0.1 mm/rev using a 9.52 mm diameter uncoated solid carbide two-fluted twist drill. They showed that the mean thrust forces in the aluminum constituent were similar (~400 N) irrespective of the cooling mode, while only flood cooling resulted in higher mean thrust force (~225 N) in the CFRP constituent compared to the mean value (~150 N) achieved with the other cooling modes. Comparable tool temperatures (~350 °C) at the exit hole were found when drilling in dry or MQL(LP-HF) conditions, while MQL(HP-LF) promoted lower temperature (~200 °C). The authors assumed that high pressure projected faster oil droplets, enhancing the penetration of coolant into the cutting area and thus reducing the friction-induced heat. No significant effect of the cooling mode on the surface roughness R_a measured in the hole wall of either the CFRP or aluminum layer was clearly identified, and the best results were obtained in dry conditions. The lowest diameter errors in CFRP and aluminum holes were achieved with flood cooling, followed by MQL(HP-LF), while the dry mode-induced holes exceeded the diameter tolerance, particularly for the aluminum constituent. Moreover, the authors stated that the two MQL modes had a negative impact on the occurrence of entry delamination, while dry and flood conditions produced delamination-free holes.

Giasin et al. [107] investigated the impact of the use of cryogenic LN_2 and MQL coolants on the entrance and exit aluminum burr size and the deviation of nominal hole size when drilling GLARE 2B 11/10-0.4 (7.1304 mm total thickness) at various spindle speeds (3000, 6000 and 9000 rpm) and feed speeds (300, 600, 900 mm/min) using a 6 mm diameter coated carbide drill with a 30° helix angle and a 140° point angle. They reported that cooling modes significantly impacted the burr size measured at the entrance and exit of the drilled holes, since the use of cutting fluids aimed to reduce the temperature during the drilling operation, which involved the lessening of the plastic deformation of the material and thus a decrease in burr formation. Thinner entrance and exit burrs were generated under MQL and cryogenic conditions compared to those observed in dry conditions. Indeed, the performance of MQL coolant, with a reduction in the entrance burr thickness of up to 50% compared to dry drilling, was better than that of cryogenic coolant, the reduction in which achieved up to 28%. Furthermore, a sharper reduction in exit burr thickness was found when drilling at high spindle speeds or high feed rates. The influence of cooling modes on burr height, which was more substantial at high spindle speeds and low feed rates, was found to be opposite depending on the position of the drilled layer (first or last aluminum layer, corresponding to the entrance or exit of the GLARE composite, respectively). Regardless of the cooling mode, the authors stated that the entrance burr height increased significantly (up to 175 and 228% for MQL and LN_2 coolants, respectively), while smaller exit burrs were observed compared to those produced in dry conditions. The selection of cooling technology also impacted the hole size at the top and bottom positions, while entrance and exit hole diameters were almost always found to be close to the nominal diameter but undersized when drilling in dry conditions due to the thermal

expansion of the constituents during the process and their relaxation after the process. Under MQL and cryogenic conditions, entrance holes were always oversized, while exit holes were either undersized under MQL conditions or also oversized when a cryogenic fluid was applied. The use of MQL coolant only affected entrance holes, changing from an undersized diameter to an oversized one, which can be attributed to the way that the coolant with limited cooling capacity was applied, only delaying the thermal expansion at the top of the GLARE composite. In contrast, both entrance and exit hole diameters became oversized in the case of the application of LN_2 coolant, the high cooling capacity of which delayed the thermal expansion and increased the epoxy matrix stiffness and the rigidity of the fibers, leading to a reduction in the fiber deflections and preventing the laminate layers from shrinking after thermal expansion. Giasin et al. [204] completed their previous investigation [107] by studying the influence of the use of cryogenic LN_2 and MQL coolants on thrust force and surface roughness when drilling the same GLARE grade with the same cutting parameters and tool as previously used. They reported that the cryogenic environment had a negative impact on the magnitude of both thrust force and torque components, which could increase by up to 20% compared to that measured when drilling under dry and MQL conditions. On the other hand, the lowest surface roughness was achieved under cryogenic conditions when drilling at low feed rates and high spindle speeds. The authors reported that the MQL strategy was also a suitable solution to promote better surface roughness inside the hole drilled in the GLARE material since these two cooling modes improved the hole wall surface quality by up to 44% over dry conditions.

4. Conclusions and Future Scope

This article provides the first comprehensive and detailed literature review on recent outstanding advances in one-shot drilling of FRP/Al stacks and FML composites under dry conditions. It addresses the key mechanisms that give rise to the main issues occurring when drilling hybrid composite stacks. This literature review also focuses on available techniques commonly used to monitor and assess overall drilled-hole quality, as well as on promising technological solutions and strategies recommended to achieve high-quality delamination-free drilled holes. Based on the exhaustive analysis of experimental investigations, mostly performed over the last past decade, several conclusions and prospects for future research works can be highlighted and summarized as follows:

- Hybrid composite stacks, including CFRP/Al assemblies and FML composites, are increasingly employed in the manufacturing of structural components in the aerospace and aeronautics industries due to their enhanced mechanical and physical properties. Additionally, these new hybrid materials are usually bolted or riveted and thus required to be drilled in a single-shot operation and under dry conditions for both environmental and economic considerations. Unfortunately, laminated composites and aluminum alloys exhibit different properties, which complicate their simultaneous drilling and induce crippling issues such as severe tool wear, heat-induced damage, drilled-hole deviations or metal burr formation.
- Delamination, fiber breakage and hole wall damage due to metal chip transport through the FRP layer, exit burrs in the aluminum layer and hole size and geometrical errors in both constituents are the main hole defects induced by the drilling of CFRP/Al stacks and FML composites. The achievement of better drilling performance of aerospace assemblies requires monitoring and assessing both offline and online parameters with well-known devices such as optical microscopes, surface profilometers, coordinate measuring machines, piezoelectric dynamometers or thermocouples. Offline parameters, such as delamination, hole wall surface roughness, hole circularity error, hole size deviation and burr height, inform on the overall quality of the drilled hole, while online parameters, such as both cutting force temperatures, constitute major indicators related to drilling defects or tool wear.
- The stringent requirements of the aerospace industry for the drilled-hole quality of CFRP/Al stacks and FML composites are required to suppress exit aluminum

burrs, minimize drilled-hole wall surface roughness and peripherical hole delamination and control the hole diameter deviation and geometrical accuracy. Numerous investigations have shown that the cutting parameters, cutting tool and cutting environment significantly influence the overall drilling performance, and optimized strategies or alternative drilling techniques should be developed to achieve high-quality delamination-free drilled holes.

- Cutting parameters represent key factors in the drilling of hybrid composite stacks since they directly impact delamination, hole surface roughness, dimensional accuracy, burr formation, drilling forces, thermal aspects, tool wear and chip formation and thus influence the drilling performance of aerospace assemblies. Generally, the feed rate was found to significantly influence cutting forces, metal chip morphology, drilled-hole wall roughness and the hole diameter of each constituent, while the choice of spindle speed had a negligible effect when drilling CFRP/Al stacks. Moreover, a reduction in the delamination extent and a rise in cutting temperature were observed when increasing cutting speed or decreasing the feed rate. Conversely, spindle speed and feed speed significantly influence cutting forces, drilled-hole wall surface roughness and burr size when drilling GLARE composites. Hence, the combination of low feed speed and low or moderate spindle speed is recommended to achieve minimum roughness, better surface finish and good hole quality, while cutting forces can be minimized when drilling with higher spindle speed.
- Tool characteristics and tool coating are other key factors in the drilling of CFRP/Al stacks and FML composites, which need to be carefully selected in order to drill high-quality holes and enhance tool life without increasing manufacturing costs. Cemented and tungsten carbide tools are preferred to HSS tools due to their better performance, even at high temperatures. The deposition of a coating layer generally delays tool wear and extends tool life. Nano- and diamond-coated drills cause a significant reduction in thrust forces and achieve lower hole wall surface roughness, while TiAlCrN and AlTiSiN-G coatings are inefficient in terms of tool wear prevention. Moreover, wear mechanisms are different depending on the type of tool coating. TiAlN-coated tools are essentially affected by abrasion, while DLC-coated drills exhibit chipping, edge rounding and abrasion. DLC coating allows the achievement of a lower delamination factor than TiAlN coating.
- Drill bit morphologies and geometries also affect hole surface quality, delamination and tool performance. Double cone, brad and spur and step drills allow thrust forces to be reduced. The brad and spur drill can also improve hole accuracy and achieve lower surface roughness, while a double cone drill is found to decrease the hole wall surface roughness compared to the conventional twist drill. Nevertheless, the conventional twist drill remains the tool commonly used when drilling CFRP/Al stacks and FML composites. Hence, significant efforts are made to optimize the characteristic angles of the twist drill to promote high-quality holes. The point angle influences thrust force and delamination. Lower values of this angle reduce delamination damage but increase thrust forces. Smaller thrust forces are produced when decreasing the clearance and chisel edge angles, while smoother surface roughness is achieved when increasing the chisel edge angle or decreasing the clearance angle. The combination of a 45° chisel edge angle, 7° primary clearance angle and 130° point angle is recommended to achieve minimum thrust force and the best hole surface roughness when drilling CFRP/AA7075-T6 stacks in a single-shot process.
- Vibration-assisted drilling and orbital drilling are two emerging drilling techniques for CFRP/Al stacks and FML composites, and promising results are found concerning the reduction in the delamination extent, the lessening of thrust forces, the decrease in cutting temperatures and the improvement of the fragmentation and evacuation of metal chips. For the VAD process, the vibration amplitude constitutes the key parameter influencing the overall drilled-hole quality and tool wear, while frequency seems to play no role.

- The performance of MQL and cryogenic cooling is still too little studied in the context of CFRP/Al stack and FML composite drilling. However, the few studies conducted show that tool wear is delayed and hole diameter deviations are reduced by MQL cooling strategies, while it seems to have a negative impact on the occurrence of entry delamination. Cryogenic cooling was exclusively investigated by one research team when drilling GLARE composites, and excellent results were found.
- This literature review shows that few investigations still exist on drilling temperatures or tool wear progression when drilling CFRP/Al stacks, while studies on the influence of cutting parameters are numerous. Further investigations should be performed on the optimization of the tool geometry by focusing on the relationship between cutting mechanisms, induced defects and the functional of the main geometrical characteristics of the drill. Furthermore, the drilling of CARALL and GLARE composites is not sufficiently studied, and more research projects in this area should be developed in the future.
- Numerical studies on the drilling of CFRP/Al stacks and FML composites are not discussed in the present article since this extensive review study focused only on the significant contributions of experimental investigations and studies. However, the authors are convinced that the selection of strategies for high-performance drilling of multi-material stacks could be optimized more efficiently by combining numerical methodologies with experimental studies. Few numerical studies on the drilling of CFRP/Al stacks and FML composites are currently available in the scientific literature, and this is a promising line of thought for forthcoming research works.

Author Contributions: Conceptualization, G.F. and P.V.; methodology, G.F.; investigation, G.F.; resources, G.F.; data curation, G.F.; writing—original draft preparation, G.F.; writing—review and editing, G.F., P.V. and M.H.H.; visualization, G.F.; supervision, G.F.; project administration, G.F.; funding acquisition, G.F. and P.V. All authors have read and agreed to the published version of the manuscript.

Funding: This research received no external funding.

Data Availability Statement: Not applicable.

Conflicts of Interest: The authors declare no conflict of interest. The funders had no role in the design of the study; in the collection, analyses or interpretation of data; in the writing of the manuscript; or in the decision to publish the results.

References

1. Khashaba, U.A. Drilling of polymer matrix composites: A review. *J. Compos. Mater.* **2012**, *47*, 1817–1832. [CrossRef]
2. Kuo, C.L.; Soo, S.L.; Aspinwall, D.K.; Carr, C.; Bradley, S.; M'Saoubi, R.; Leahy, W. Development of single step drilling technology for multilayer metallic-composite stacks using uncoated and PVD coated carbide tools. *J. Manuf. Process.* **2018**, *31*, 286–300. [CrossRef]
3. Xu, J.; Mkaddem, A.; El Mansori, M. Recent advances in drilling hybrid FRP/Ti composite: A state-of-the-art review. *Compos. Struct.* **2016**, *135*, 316–338. [CrossRef]
4. Liang, X.; Wu, D.; Gao, Y.; Chen, K. Investigation on the non-coaxiality in the drilling of carbon-fibre-reinforced plastic and aluminium stacks. *Int. J. Mach. Tools Manuf.* **2018**, *125*, 1–10. [CrossRef]
5. Singh, A.P.; Sharma, M.; Singh, I. A review of modelling and control during drilling of fiber reinforced plastic composites. *Compos. B Eng.* **2013**, *47*, 118–125. [CrossRef]
6. Mouritz, A.P. *Introduction to Aerospace Materials*; Woodhead Publishing: Sawaston, UK, 2012.
7. Zitoune, R.; Krishnaraj, V.; Collombet, F. Study of drilling of composite material and aluminium stack. *Compos. Struct.* **2010**, *92*, 1246–1255. [CrossRef]
8. Ashrafi, S.A.; Sharif, S.; Farid, A.A.; Yahya, M.Y. Performance evaluation of carbide tools in drilling CFRP-Al stacks. *J. Compos. Mater.* **2014**, *48*, 2071–2084. [CrossRef]
9. Vlot, A.; Gunnink, J.W. *Fibre Metal Laminates: An Introduction*, 1st ed.; Kluwer Academic Publishers: Dordrecht, The Netherland, 2001.
10. Wu, G.; Yang, J.M. The mechanical behavior of GLARE laminates for aircraft structures. *JOM* **2005**, *57*, 72–79. [CrossRef]
11. Bonhin, E.P.; David-Müzel, S.; de Sampaio Alves, M.C.; Botelho, E.C.; Ribeiro, M.V. A review of mechanical drilling on fiber metal laminates. *J. Compos. Mater.* **2020**, *55*, 843–869. [CrossRef]

12. Kuo, C.L.; Soo, S.L.; Aspinwall, D.K.; Thomas, W.; Bradley, S.; Pearson, D.; M'Saoubi, R.; Leahy, W. The effect of cutting speed and feed rate on hole surface integrity in single-shot drilling of metallic-composite stacks. *Procedia CIRP* **2014**, *13*, 405–410. [CrossRef]
13. Aamir, M.; Tolouei-Rad, M.; Giasin, K.; Nosrati, A. Recent advances in drilling of carbon fiber–reinforced polymers for aerospace applications: A review. *Int. J. Adv. Manuf. Technol.* **2019**, *105*, 2289–2308. [CrossRef]
14. Klocke, F.; Eisenblätter, G. Dry cutting. *CIRP Ann.* **1997**, *46*, 519–526. [CrossRef]
15. Batzer, S.; Haan, D.; Rao, P.; Olson, W.; Sutherland, J. Chip morphology and hole surface texture in the drilling of cast aluminum alloys. *J. Mater. Process. Technol.* **1998**, *79*, 72–78. [CrossRef]
16. Sreejith, P.; Ngoi, B. Dry machining: Machining of the future. *J. Mater. Process. Technol.* **2000**, *101*, 287–291. [CrossRef]
17. Dixit, U.S.; Sarma, D.K.; Davim, J.P. *Environmentally Friendly Machining*; Springer: Berlin/Heidelberg, Germany, 2012.
18. Liu, D.; Tang, Y.; Cong, W.L. A review of mechanical drilling for composite laminates. *Compos. Struct.* **2012**, *94*, 1265–1279. [CrossRef]
19. Shyha, I.S.; Aspinwall, D.K.; Soo, S.L.; Bradley, S. Drill geometry and operating effects when cut-ting small diameter holes in CFRP. *Int. J. Mach. Tools Manuf.* **2009**, *49*, 1008–1114. [CrossRef]
20. Abrão, A.M.; Faria, P.E.; Rubio, J.C.C.; Reis, P.; Davim, J.P. Drilling of fiber reinforced plastics: A review. *J. Mater. Process. Technol.* **2007**, *186*, 1–7. [CrossRef]
21. Dandekar, C.R.; Shin, Y.C. Modeling of machining of composite materials: A review. *Int. J. Mach. Tools Manuf.* **2012**, *57*, 102–121. [CrossRef]
22. Ben Soussia, A.; Mkaddem, A.; El Mansori, M. Rigorous treatment of dry cutting of FRP—Interface consumption concept: A review. *Int. J. Mech. Sci.* **2014**, *83*, 1–29. [CrossRef]
23. Che, D.; Saxena, I.; Han, P.; Guo, P.; Ehmann, K.F. Machining of Carbon Fiber Reinforced Plastics/Polymers: A literature review. *J. Manuf. Sci. Eng.* **2014**, *136*, 34001. [CrossRef]
24. Kumar, D.; Singh, K.K. An approach towards damage free machining of CFRP and GFRP composite material: A review. *Adv. Compos. Mater.* **2015**, *24*, 49–63. [CrossRef]
25. M'Saoubi, R.; Axinte, D.; Soo, S.L.; Nobel, C.; Attia, H.; Kappmeyer, G.; Engin, S.; Sim, W.-M. High performance cutting of advanced aerospace alloys and composite materials. *CIRP Ann.* **2015**, *64*, 557–580. [CrossRef]
26. Shetty, N.; Shahabaz, S.M.; Sharma, S.S.; Shetty, S.D. A review on finite element method for machining of composite materials. *Compos. Struct.* **2017**, *176*, 790–802. [CrossRef]
27. Karataş, M.A.; Gökkaya, H. A review on machinability of carbon fiber reinforced polymer (CFRP) and glass fiber reinforced polymer (GFRP) composite materials. *Def. Technol.* **2018**, *14*, 318–326. [CrossRef]
28. Panchagnula, K.K.; Palaniyandi, K. Drilling on fiber reinforced polymer/nanopolymer composite laminates: A review. *J. Mater. Res. Technol.* **2018**, *7*, 180–189. [CrossRef]
29. Vigneshwaran, S.; Uthayakumar, M.; Arumugaprabu, V. Review on machinability of fiber reinforced polymers: A drilling approach. *Silicon* **2018**, *10*, 2295–2305. [CrossRef]
30. Wang, G.-D.; Melly, S.K. Three-dimensional finite element modeling of drilling CFRP composites using Abaqus/CAE: A review. *Int. J. Adv. Manuf. Technol.* **2018**, *94*, 599–614. [CrossRef]
31. Geng, D.; Liu, Y.; Shao, Z.; Lu, Z.; Cai, J.; Li, X.; Jiang, X.; Zhang, D. Delamination formation, evaluation and suppression during drilling of composite laminates: A review. *Compos. Struct.* **2019**, *216*, 168–186. [CrossRef]
32. John, K.M.; Kumaran, S.T.; Kurniawan, R.; Park, K.M.; Byeon, J.H. Review on the methodologies adopted to minimize the material damages in drilling of carbon fiber reinforced plastic composites. *J. Reinf. Plast. Compos.* **2019**, *38*, 351–368. [CrossRef]
33. Cepero-Mejias, F.; Curiel-Sosa, J.L.; Blazquez, A.; Yu, T.T.; Kerrigan, K.; Phadnis, V.A. Review of recent developments and induced damage assessment in the modelling of the machining of long fibre reinforced polymer composites. *Compos. Struct.* **2020**, *240*, 112006. [CrossRef]
34. Zadafiya, K.; Bandhu, D.; Kumari, S.; Chatterjee, S.; Abhishek, K. Recent trends in drilling of carbon fiber reinforced polymers (CFRPs): A state-of-the-art review. *J. Manuf. Process.* **2021**, *69*, 7–68. [CrossRef]
35. Wang, X.; Wang, F.; Gu, T.; Jia, Z.; Shi, Y. Computational simulation of the damage response for machining long fibre reinforced plastic (LFRP) composite parts: A review. *Compos. Part A Appl. Sci. Manuf.* **2021**, *143*, 106296. [CrossRef]
36. Poor, D.; Geier, N.; Pereszlai, C.; Xu, J. A critical review of the drilling of CFRP composites: Burr formation, characterisation and challenges. *Compos. B Eng.* **2021**, *223*, 109155. [CrossRef]
37. Du, J.; Geng, M.; Ming, W.; He, W.; Ma, J. Simulation machining of fiber-reinforced composites: A review. *Int. J. Adv. Manuf. Technol.* **2021**, *117*, 1–15. [CrossRef]
38. Chen, Y.; Yang, H.; Xu, J.; Fu, Y.; Yan, C. Recent advances in hole making of FRP/metal stacks: A review. *Trans. Nanjing Univ. Aeronaut. Astronaut.* **2019**, *36*, 361–375.
39. Kim, D.; Ramulu, M. Drilling process optimization for graphite/bismaleimide–titanium alloy stacks. *Compos. Struct.* **2004**, *63*, 101–114. [CrossRef]
40. Feito, N.; Muñoz-Sánchez, A.; Díaz-Álvarez, A.; Miguelez, M.H. Multi-objective optimization analysis of cutting parameters when drilling composite materials with special geometry drills. *Compos. Struc.* **2019**, *225*, 111187. [CrossRef]
41. Gu, W.; Xu, H.; Liu, J.; Yue, Z. Effect of drilling process on fatigue life of open holes. *Tsinghua Sci. Technol.* **2009**, *14*, 54–57. [CrossRef]

42. Liu, J.; Xu, H.; Zhai, H.; Yue, Z. Effect of detail design on fatigue performance of fastener hole. *Mater. Des.* **2010**, *31*, 976–980. [CrossRef]
43. Wang, G.-D.; Melly, S.K.; Li, N.; Peng, T.; Li, Y. Research on milling strategies to reduce delamination damage during machining of holes in CFRP/Ti stack. *Compos. Struc.* **2018**, *200*, 679–688. [CrossRef]
44. El-Sonbaty, I.; Khashaba, U.A.; Machaly, T. Factors affecting the machinability of GFR/epoxy composites. *J. Compos. Struct.* **2004**, *63*, 329–338. [CrossRef]
45. Khashaba, U.A.; El-Sonbaty, I.; Selmy, A.I.; Megahed, A.A. Machinability analysis in drilling woven GFR/epoxy composites: Part I—Effect of machining parameters. *Compos. A Appl. Sci. Manuf.* **2010**, *41*, 391–400. [CrossRef]
46. Kavad, B.V.; Pandey, A.B.; Tadavi, M.V.; Jakharia, H.C. A review paper on effects of drilling on glass fiber reinforced plastic. *Proc. Technol.* **2014**, *14*, 457–464. [CrossRef]
47. Park, K.-H.; Beal, A.; Kim, D.; Kwon, P.; Lantrip, J. Tool wear in drilling of composite/titanium stacks using carbide and polycrystalline diamond tools. *Wear* **2011**, *271*, 2826–2835. [CrossRef]
48. Brinksmeier, E.; Janssen, R. Drilling of multi-layer composite materials consisting of carbon fiber reinforced plastics (CFRP), titanium and aluminum Alloys. *CIRP Ann.* **2002**, *51*, 87–90. [CrossRef]
49. Montoya, M.; Calamaz, M.; Gehin, D.; Girot, F. Evaluation of the performance of coated and uncoated carbide tools in drilling thick CFRP/aluminium alloy stacks. *Int. J. Adv. Manuf. Technol.* **2013**, *68*, 2111–2120. [CrossRef]
50. Ismail, S.O.; Dhakal, H.N.; Popov, I.; Beaugrand, J. Comprehensive study on machinability of sustainable and conventional fibre reinforced polymer composites. *Eng. Sci. Technol. Int. J.* **2016**, *19*, 2043–2052. [CrossRef]
51. Caprino, G.; Tagliaferri, V. Damage development in drilling glass fiber reinforced plastics. *Int. J. Mach. Tools Manuf.* **1995**, *35*, 817–829. [CrossRef]
52. Murphy, C.; Byrne, G.; Gilchrist, M.D. The performance of coated tungsten carbide drills when machining carbon fibre-reinforced epoxy composite materials. *Proc. Inst. Mech. Eng. Part B* **2002**, *216*, 143–152. [CrossRef]
53. Davim, J.; Reis, P. Study of delamination in drilling carbon fiber reinforced plastics (CFRP) using design experiments. *Compos. Struct.* **2003**, *59*, 481–487. [CrossRef]
54. Gaitonde, V.N.; Karnik, S.R.; Davim, J.P. Prediction and minimization of delamination in drilling of medium density fiberboard (MDF) using response surface methodology and Taguchi design. *Mater. Manuf. Process.* **2008**, *23*, 377–384. [CrossRef]
55. Rubio, J.C.; Abrão, A.M.; Faria, P.E.; Correia, A.E.; Davim, J.P. Effects of high speed in the drilling of glass fibre reinforced plastic: Evaluation of the delamination factor. *Int. J. Mach. Tools Manuf.* **2008**, *48*, 715–720. [CrossRef]
56. Rajamurugan, T.V.; Shanmugam, K.; Palanikumar, K. Analysis of delamination in drilling glass fiber reinforced polyester composites. *Mater. Des.* **2013**, *45*, 80–87. [CrossRef]
57. Gaugel, S.; Sripathy, P.; Haeger, A.; Meinhard, D.; Bernthaler, T.; Lissek, F.; Kaufeld, M.; Knoblauch, V.; Schneider, G. A comparative study on tool wear and laminate damage in drilling of carbon-fiber reinforced polymers (CFRP). *Compos. Struct.* **2016**, *155*, 173–183. [CrossRef]
58. Haeger, A.; Schoen, G.; Lissek, F.; Meinhard, D.; Kaufeld, M.; Schneider, G.; Schuhmacher, S.; Knoblauch, V. Non-destructive detection of drilling-induced delamination in CFRP and its effect on mechanical properties. *Procedia Eng.* **2016**, *149*, 130–142. [CrossRef]
59. Hrechuk, A.; Bushlya, V.; Ståhl, J. Hole-quality evaluation in drilling fiber-reinforced composites. *Compos. Struct.* **2018**, *204*, 378–387. [CrossRef]
60. Khashaba, U.A. Delamination in drilling GFR-thermoset composites. *Compos. Struct.* **2004**, *63*, 313–327. [CrossRef]
61. Davim, J.; Rubio, J.; Abrão, A. A novel approach based on digital image analysis to evaluate the delamination factor after drilling composite laminates. *Compos. Sci. Technol.* **2007**, *67*, 1939–1945. [CrossRef]
62. Faraz, A.; Biermann, D.; Weinert, K. Cutting edge rounding: An innovative tool wear criterion in drilling CFRP composite laminates. *Int. J. Mach. Tools. Manuf.* **2009**, *49*, 1185–1196. [CrossRef]
63. Durão, L.M.; Gonçalves, D.J.; Tavares, J.M.R.; de Albuquerque, V.H.C.; Vieira, A.A.; Marques, A.T. Drilling tool geometry evaluation for reinforced composite laminates. *Compos. Struct.* **2010**, *92*, 1545–1550. [CrossRef]
64. Durão, L.M.; Tavares, M.R.; de Albuquerque, V.H.C. Damage evaluation of drilled carbon/epoxy laminates based on area assessment methods. *Compos. Struct.* **2013**, *96*, 576–583. [CrossRef]
65. Silva, D.; Teixeira, J.P.; Machado, C.M. Methodology analysis for evaluation of drilling induced damage in composites. *Int. J. Adv. Manuf. Technol.* **2014**, *71*, 1919–1928. [CrossRef]
66. Tsao, C.C.; Hocheng, H. Taguchi analysis of delamination associated with various drill bits in drilling of composite material. *Int. J. Mach. Tools Manuf.* **2004**, *44*, 1085–1090. [CrossRef]
67. Tsao, C.C.; Hocheng, H. Computerized tomography and C-Scan for measuring delamination in the drilling of composite materials using various drills. *Int. J. Mach. Tools Manuf.* **2005**, *45*, 1282–1287. [CrossRef]
68. Hocheng, H.; Tsao, C.C. Computerized tomography and C-scan for measuring drilling-induced delamination in composite material using twist drill and core drill. *Key. Eng. Mater.* **2007**, *339*, 16–20. [CrossRef]
69. Tsao, C.C.; Kuo, K.L.; Hsu, I.C. Evaluation of a novel approach to a delamination factor after drilling composite laminates using a core–saw drill. *Int. J. Adv. Manuf. Technol* **2012**, *59*, 617–622. [CrossRef]
70. Tsao, C.C.; Hocheng, H.; Chen, Y.C. Delamination reduction in drilling composite materials by active backup force. *CIRP Ann. Manuf. Technol.* **2012**, *61*, 91–94. [CrossRef]

71. Xu, J.; Li, C.; Mi, S.; An, Q.; Chen, M. Study of drilling-induced defects for CFRP composites using new criteria. *Compos. Struct.* **2018**, *201*, 1076–1087. [CrossRef]
72. Chen, W.C. Some experimental investigations in the drilling of carbon fiber-reinforced plastic (CFRP) composite laminates. *Int. J. Mach. Tools. Manuf.* **1997**, *37*, 1097–1108. [CrossRef]
73. Saoudi, J.; Zitoune, R.; Mezlini, S.; Gururaja, S.; Seitier, P. Critical thrust force predictions during drilling: Analytical modeling and X-ray tomography quantification. *Compos. Struct.* **2016**, *153*, 886–894. [CrossRef]
74. Xu, J.; An, Q.; Cai, X.; Chen, M. Drilling machinability evaluation on new developed high-strength T800S/250F CFRP laminates. *Int. J. Precis. Eng. Manuf.* **2013**, *14*, 1687–1696. [CrossRef]
75. Mohan, N.S.; Kulkarni, S.M.; Ramachandra, A. Delamination analysis in drilling process of glass fiber reinforced plastic (GFRP) composite materials. *J. Mater. Process. Technol.* **2007**, *186*, 265–271. [CrossRef]
76. Nagarajan, V.A.; Selwin Rajadurai, J.; Annil Kumar, T.A. Digital image analysis to evaluate delamination factor for wind turbine composite laminate blade. *Compos. B. Eng.* **2012**, *43*, 3153–3159. [CrossRef]
77. Hassan, M.H.; Abdullah, J.; Franz, G. Multi-objective optimization in single-shot drilling of CFRP/Al stacks using customized twist drill. *Materials* **2022**, *15*, 1981. [CrossRef]
78. Giasin, K.; Ayvar-Soberanis, S.; Hodzic, A. An experimental study on drilling of unidirectional GLARE fibre metal laminates. *Compos. Struct.* **2015**, *133*, 794–808. [CrossRef]
79. Palanikumar, K.; Karunamoorthy, L.; Karthikeyan, R. Assessment of factors influencing surface roughness on the ma-chining of glass fiber-reinforced polymer composites. *Mater. Des.* **2006**, *27*, 862–871. [CrossRef]
80. Kurt, M.; Kaynac, Y.; Bagci, E. Evaluation of drilled hole quality in Al 2024 alloy. *Int. J. Adv. Manuf. Technol.* **2008**, *37*, 1051–1060. [CrossRef]
81. Krishnaraj, V.; Prabukarthi, A.; Ramanathan, A.; Elanghovan, N.; Kumar, M.S.; Zitoune, R.; Davim, J. Optimization of machining parameters at high speed drilling of carbon fiber reinforced plastic (CFRP) laminates. *Compos. Part B Eng.* **2012**, *43*, 1791–1799. [CrossRef]
82. Sui, S.; Song, G.; Sun, C.; Zhu, Z.; Guo, K.; Sun, J. Experimental investigation on the performance of novel double cone integrated tool in one-shot drilling of metal stacks. *Int. J. Adv. Manuf. Technol.* **2020**, *109*, 523–534. [CrossRef]
83. Mahdi, A.; Turki, Y.; Habak, M.; Salem, M.; Bouaziz, Z. Experimental study of thrust force and surface quality when drilling hybrid stacks. *Int. J. Adv. Manuf. Technol.* **2020**, *107*, 3981–3994. [CrossRef]
84. Jia, Z.-Y.; Zhang, C.; Wang, F.-J.; Fu, R.; Chen, C. Multi-margin drill structure for improving hole quality and dimensional consistency in drilling Ti/CFRP stacks. *J. Mater. Process. Technol.* **2020**, *276*, 116405. [CrossRef]
85. Ghidossi, P.; El Mansori, M.; Pierron, F. Edge machining effects on the failure of polymer matrix composite coupons. *Compos. A* **2004**, *35*, 989–999. [CrossRef]
86. König, W.; Graß, P. Quality definition and assessment in drilling of fibre reinforced thermosets. *CIRP Ann.* **1989**, *38*, 119–124. [CrossRef]
87. Wang, C.-Y.; Chen, Y.-H.; An, Q.-L.; Cai, X.-J.; Ming, W.-W.; Chen, M. Drilling temperature and hole quality in drilling of CFRP/aluminum stacks using diamond coated drill. *Int. J. Precis. Eng.* **2015**, *16*, 1689–1697. [CrossRef]
88. Zhang, L.; Liu, Z.; Tian, W.; Liao, W. Experimental studies on the performance of different structure tools in drilling CFRP/Al alloy stacks. *Int. J. Adv. Manuf. Technol.* **2015**, *81*, 241–251. [CrossRef]
89. Shilpa, M.K.; Yendapalli, V. Surface roughness estimation techniques for drilled surfaces: A review. *Mater. Today Proc.* **2022**, *52*, 1082–1091. [CrossRef]
90. Zitoune, R.; Krishnaraj, V.; Almabouacif, B.S.; Collombet, F.; Sima, M.; Jolin, A. Influence of machining parameters and new nano-coated tool on drilling performance of CFRP/Aluminium sandwich. *Compos. Part B Eng.* **2012**, *43*, 1480–1488. [CrossRef]
91. Shyha, I.S.; Soo, S.L.; Aspinwall, D.K.; Bradley, S.; Perry, R.; Harden, P.; Dawson, S. Hole quality assessment following drilling of metallic-composite stacks. *Int. J. Mach. Tools Manuf.* **2011**, *51*, 569–578. [CrossRef]
92. Zitoune, R.; Cadorin, R.; Elambouacif, B.S.; Collombet, F.; Krishnaraj, V.; Bougherara, H. Influence of the double cone drill geometry on the holes quality during drilling multi-stack made of CFRP/Al. *Int. J. Mater Mech. Manuf.* **2014**, *2*, 292–296.
93. Meshreki, M.; Damir, A.; Sadek, A.; Attia, M.H. Investigation of drilling of CFRP-Aluminum stack under different cooling modes. In Proceedings of the ASME International Mechanical Engineering Congress and Exposition, Phoenix, AZ, USA, 11–17 November 2016.
94. Zitoune, R.; Krishnaraj, V.; Collombet, F.; Le Roux, S. Experimental and numerical analysis on drilling of carbon fibre reinforced plastic and aluminium stacks. *Compos. Struct.* **2016**, *146*, 148–158. [CrossRef]
95. Hassan, M.H.; Abdullah, J.; Mahmud, A.S.; Supran, A. Effects of twist drill geometry and drilling parameters on CFRP-aluminum stack up in single shot drilling. *SciFed Mater. Res. Lett.* **2018**, *2*, 1–14.
96. Bañon, F.; Sambruno, A.; Fernández-Vidal, S.; Fernández-Vidal, S.R. One-shot drilling analysis of stack CFRP/UNS A92024 bonding by adhesive. *Materials* **2019**, *12*, 160. [CrossRef] [PubMed]
97. Janakiraman, A.; Pemmasani, S.; Sheth, S.; Kannan, C. Experimental investigation and parametric optimization on hole quality assessment during drilling of CFRP/GFRP/Al stacks. *J. Inst. Eng. India Ser. C* **2020**, *101*, 291–302. [CrossRef]
98. Hassan, M.; Abdullah, J.; Franz, G.; Shen, C.; Mahmoodian, R. Effect of twist drill geometry and drilling parameters on hole quality in single-shot drilling of CFRP/Al7075-T6 Composite Stack. *J. Compos. Sci.* **2021**, *5*, 189. [CrossRef]

99. Giasin, K.; Ayvar-Soberanis, S. An Investigation of burrs, chip formation, hole size, circularity and delamination during drilling operation of GLARE using ANOVA. *Compos. Struct.* **2017**, *159*, 745–760. [CrossRef]
100. Park, S.Y.; Choi, W.J.; Choi, C.H.; Choi, H.S. Effect of drilling parameters on hole quality and delamination of hybrid GLARE laminate. *Compos. Struct.* **2018**, *185*, 684–698. [CrossRef]
101. Giasin, K.; Gorey, G.; Byrne, C.; Sinke, J.; Brousseau, E. Effect of machining parameters and cutting tool coating on hole quality in dry drilling of fibre metal laminates. *Compos. Struct.* **2019**, *212*, 159–174. [CrossRef]
102. Bolar, G.; Sridhar, A.K.; Ranjan, A. Drilling and helical milling for hole making in multi-material carbon reinforced aluminum laminates. *Int. J. Lightweight Mater. Manuf.* **2022**, *5*, 113–125. [CrossRef]
103. Kuo, C.; Li, Z.; Wang, C. Multi-objective optimisation in vibration-assisted drilling of CFRP/Al stacks. *Compos. Struct.* **2017**, *173*, 196–209. [CrossRef]
104. D'Orazio, A.; El Mehtedi, M.; Forcellese, A.; Nardinocchi, A.; Simoncini, M. Tool wear and hole quality in drilling of CFRP/AA7075 stacks with DLC and nanocomposite TiAlN coated tools. *J. Manuf. Process.* **2017**, *30*, 582–592. [CrossRef]
105. Ekici, E.; Motorcu, A.R.; Yildirim, E. An experimental study on hole quality and different delamination approaches in the drilling of CARALL, a new FML composite. *FME Trans.* **2021**, *49*, 950–961. [CrossRef]
106. Zhang, H.; Dang, J.; An, Q.; Cai, X.; Chen, M. Study on the drilling performances of a newly developed CFRP/invar co-cured material. *J. Manuf. Process.* **2021**, *66*, 669–678. [CrossRef]
107. Giasin, K.; Ayvar-Soberanis, S.; Hodzic, A. The effects of minimum quantity lubrication and cryogenic liquid nitrogen cooling on drilled hole quality in GLARE fibre metal laminates. *Mater. Des.* **2016**, *89*, 996–1006. [CrossRef]
108. Giasin, K.; Hawxwell, J.; Sinke, J.; Dhakal, H.; Köklü, U.; Brousseau, E. The effect of cutting tool coating on the form and dimensional errors of machined holes in GLARE fibre metal laminates. *Int. J. Adv. Manuf. Technol.* **2020**, *107*, 2817–2832. [CrossRef]
109. Seeholzer, L.; Voss, R.; Marchetti, L.; Wegener, K. Experimental study: Comparison of conventional and low-frequency vibration-assisted drilling (LF-VAD) of CFRP/aluminium stacks. *Int. J. Adv. Manuf. Technol.* **2019**, *104*, 433–449. [CrossRef]
110. Zou, F.; Dang, J.; An, Q.; Chen, M. Mechanism and feasibility study of low frequency vibration assisted drilling of a newly developed CFRP/Al co-cured material. *J. Manuf. Process.* **2021**, *68*, 115–127. [CrossRef]
111. Rivero, A.; Aramendi, G.; Herranz, S.; Lopez de Lacalle, L.N. An experimental investigation of the effect of coatings and cutting parameters on the dry drilling performance of aluminium alloys. *Int. J. Adv. Manuf. Technol.* **2006**, *28*, 1–11. [CrossRef]
112. Devitte, C.; Souza, G.S.C.; Souza, A.J.; Tita, V. Optimization for drilling process of metal composite aeronautical structures. *Sci. Eng. Compos.* **2021**, *28*, 264–275. [CrossRef]
113. Costa, E.S.; da Silva, M.B.; Machado, A.R. Burr produced on the drilling process as a function of tool wear and lubricant-coolant conditions. *J. Braz. Soc. Mech. Sci. Eng.* **2009**, *31*, 57–63. [CrossRef]
114. Avila, M.C.; Gardner, J.D.; Reich-Weiser, C.; Vijayaraghavan, A.; Dornfeld, D. Strategies for burr minimization and cleanability in aerospace and automotive manufacturing. *SAE Trans. J. Aerosp.* **2006**, *114*, 1073–1081.
115. Bu, Y.; Liao, W.H.; Tian, W.; Shen, J.X.; Hu, J. An analytical model for exit burrs in drilling of aluminum materials. *Int. J. Adv. Manuf. Tech.* **2016**, *85*, 2783–2796. [CrossRef]
116. Min, S.; Kim, J.; Dornfeld, D.A. Development of a drilling burr control chart for low alloy steel, AISI 4118. *J. Mater. Process. Technol.* **2001**, *113*, 4–9. [CrossRef]
117. Rezende, B.A.; Silveira, M.L.; Vieira, L.M.G.; Abrão, A.M.; Faria, P.E.; Rubio, J.C.C. Investigation on the effect of drill geometry and pilot holes on thrust force and burr height when drilling an aluminium/PE sandwich material. *Materials* **2016**, *9*, 774. [CrossRef] [PubMed]
118. Dong, S.; Liao, W.; Zheng, K.; Liu, J.; Feng, J. Investigation on exit burr in robotic rotary ultrasonic drilling of CFRP/aluminum stacks. *Int. J. Mech. Sci.* **2019**, *151*, 868–876. [CrossRef]
119. Möhring, H.-C.; Kimmelmann, M.; Eschelbacher, S.; Güzel, K.; Gauggel, C. Process monitoring on drilling fiber-reinforced plastics and aluminium stacks using acoustic emissions. *Procedia Manuf.* **2018**, *18*, 58–67. [CrossRef]
120. Kimmelmann, M.; Duntschew, J.; Schluchter, I.; Möhring, H.-C. Analysis of burr formation mechanisms when drilling CFRP-aluminium stacks using acoustic emission. *Procedia Manuf.* **2019**, *40*, 64–69. [CrossRef]
121. López de Lacalle, L.N.; Rivero, A.; Lamikiz, A. Mechanistic model for drills with double point-angle edges. *Int. J. Adv. Manuf. Technol.* **2009**, *40*, 447–457. [CrossRef]
122. Zitoune, R.; Collombet, F. Numerical prediction of the thrust force responsible of delamination during the drilling of the long-fibre composite structures. *Compos. A Appl. Sci.* **2007**, *38*, 858–866. [CrossRef]
123. Pardo, A.; Majeed, M.; Heinemann, R. Process signals characterisation to enable adaptive drilling of aerospace stacks. *Procedia CIRP* **2020**, *88*, 479–484. [CrossRef]
124. Fernández-Vidal, S.R.; Fernández-Vidal, S.; Batista, M.; Salguero, J. Tool wear mechanism in cutting of stack CFRP/UNS A97075. *Materials* **2018**, *11*, 1276. [CrossRef]
125. Soo, S.L.; Abdelhafeez, A.M.; Li, M.; Hood, R.; Lim, C.M. The drilling of carbon fibre composite-aluminium stacks and its effect on hole quality and integrity. *Proc. Inst. Mech. Eng. B Manag. Eng. Manufact.* **2019**, *233*, 1323–1331. [CrossRef]
126. Bonnet, C.; Poulachon, G.; Rech, J.; Girard, Y.; Costes, J.P. CFRP drilling: Fundamental study of local feed force and consequences on hole exit damage. *Int. J. Mach. Tools Manuf.* **2015**, *94*, 57–64. [CrossRef]

127. Zhong, B.; Zou, F.; An, Q.; Chen, M.; Zhang, H.; Xie, C. Experimental study on drilling process of a newly developed CFRP/Al/CFRP co-cured material. *J. Manuf. Process.* **2022**, *75*, 476–484. [CrossRef]
128. Sridhar, A.K.; Bolar, G.; Padmaraj, N.H. Comprehensive experimental investigation on drilling multi-material carbon fiber reinforced aluminum laminates. *J. King Saud Univ. Eng. Sci.* **2021**. [CrossRef]
129. Boughdiri, I.; Giasin, K.; Mabrouki, T.; Zitoune, R. Effect of cutting parameters on thrust force, torque, hole quality and dust generation during drilling of GLARE 2B laminate. *Compos. Struct.* **2021**, *261*, 113562. [CrossRef]
130. Fujishima, M.; Ohno, K.; Nishikawa, S.; Nishimura, K.; Sakamoto, M.; Kawai, K. Study of sensing technologies for machine tools. *CIRP J. Manuf. Sci. Technol.* **2016**, *14*, 71–75. [CrossRef]
131. Benezech, L.; Landon, Y.; Rubio, W. Study of manufacturing defects and tool geometry optimisation for multi-material stack drilling. *Adv. Mat. Res.* **2011**, *423*, 1–11. [CrossRef]
132. Neugebauer, R.; Ben-Hanan, U.; Ihlenfeldt, S.; Wabner, M.; Stoll, A. Acoustic emission as a tool for identifying drill position in fiber-reinforced plastic and aluminum stacks. *Int. J. Mach. Tools Manuf.* **2012**, *57*, 20–26. [CrossRef]
133. Wertheim, R.; Ben-Hanan, U.; Ihlenfeldt, S.; Stoll, A.; Treppe, F.; Wabner, M. Acoustic emission for controlling drill position in fiber-reinforced plastic and metal stacks. *CIRP Ann. Manuf. Technol.* **2012**, *61*, 75–78. [CrossRef]
134. El Bouami, S.; Habak, M.; Velasco, R.; Dos Santos, B.; Franz, G.; Vantomme, P. Tool geometry optimization for drilling CFRP/Al-Li stacks with a lightning strike protection. *AIP Conf. Proc.* **2017**, *1896*, 090009.
135. Bleicher, F.; Wiesinger, G.; Kumpf, C.; Finkeldei, D.; Baumann, C.; Lechner, C. Vibration assisted drilling of CFRP/metal stacks at low frequencies and high amplitudes. *Prod. Eng.* **2018**, *12*, 289–296. [CrossRef]
136. Wang, G.-D.; Kirwa, M.S.; Li, N. Experimental studies on a two-step technique to reduce damage during milling of large diameter holes in CFRP/Al stack delamination. *Compos. Struct.* **2018**, *188*, 330–339. [CrossRef]
137. Dang, J.; Zou, F.; Cai, X.; An, Q.; Ming, W.; Chen, M. Experimental investigation on mechanical drilling of a newly developed CFRP/Al co-cured material. *Int. J. Adv. Manuf. Technol.* **2020**, *106*, 993–1004. [CrossRef]
138. Sato, M.; Tanaka, H.; Yamamoto, K. Temperature variations in drilling of CFRP/aluminum and CFRP/titanium stacks. *Int. J. Autom. Technol.* **2016**, *10*, 348–355. [CrossRef]
139. Park, J.-M.; Kwon, D.-J.; Wang, Z.-J.; Gu, G.-Y.; DeVries, K.L. A new strategy of carbon fiber reinforced plastic drilling evaluation using thermal measurement. *J. Compos. Mater.* **2013**, *47*, 2005–2011. [CrossRef]
140. Yashiro, T.; Ogawa, T.; Sasahara, H. Temperature measurement of cutting tool and machined surface layer in milling of CFRP. *Int. J. Mach. Tools Manuf.* **2013**, *70*, 63–69. [CrossRef]
141. Rizal, M.; Ghani, J.A.; Nuawi, M.Z.; Haron, C.H.C. An embedded multi-sensor system on the rotating dynamometer for real-time condition monitoring in milling. *Int. J. Adv. Manuf. Technol.* **2018**, *95*, 811–823. [CrossRef]
142. Sheikh-Ahmad, J.Y.; Almaskari, F.; Hafeez, F. Thermal aspects in machining CFRPs: Effect of cutter type and cutting parameters. *Int. J. Adv. Manuf. Technol.* **2019**, *100*, 2569–2582. [CrossRef]
143. Pinillos, U.A.; Fernández-Vidal, S.R.; Calamaz, M.; Girot Mata, F.A. Wear mechanisms and wear model of carbide tools during dry Drilling of CFRP/TiAl6V4 Stacks. *Materials* **2019**, *12*, 2843. [CrossRef]
144. Xu, J.; Zhou, L.; Chen, M.; Ren, F. Experimental study on mechanical drilling of carbon/epoxy composite-Ti6Al4V stacks. *Mater. Manuf. Process.* **2019**, *34*, 715–725. [CrossRef]
145. Moghaddas, M.A.; Yi, A.Y.; Graff, K.F. Temperature measurement in ultrasonic-assisted drilling process. *Int. J. Adv. Manuf. Technol.* **2019**, *103*, 187–199. [CrossRef]
146. Kolesnyk, V.; Kryvoruchko, D.; Hatala, M.; Mital, D.; Hutyrova, Z.; Duplak, J.; Alowa, M. The effect of cutting temperature on carbide drilling life in the process of CFRP/steel stacks drilling. *Manuf. Technol.* **2015**, *15*, 357–362. [CrossRef]
147. Sanda, A.; Arriola, I.; Navas, V.G.; Bengoetxea, I.; Gonzalo, O. Ultrasonically assisted drilling of carbon fibre reinforced plastics and Ti6Al4V. *J. Manuf. Process.* **2016**, *22*, 169–176. [CrossRef]
148. Wei, Y.; An, Q.; Ming, W.; Chen, M. Effect of drilling parameters and tool geometry on drilling performance in drilling carbon fiber-reinforced plastic/titanium alloy stacks. *Adv. Mech. Eng.* **2016**, *8*, 1687814016670281. [CrossRef]
149. Hussein, R.; Sadek, A.; Elbestawi, M.A.; Attia, M.H. Low-frequency vibration-assisted drilling of hybrid CFRP/Ti6Al4V stacked material. *Int. J. Adv. Manuf. Technol.* **2018**, *98*, 2801–2817. [CrossRef]
150. Onawumi, P.Y.; Roy, A.; Silberschmidt, V.V.; Merson, E. Ultrasonically assisted drilling of aerospace CFRP/Ti stack. *Procedia CIRP* **2018**, *77*, 383–386. [CrossRef]
151. Wang, H.; Zhang, X.; Duan, Y. Effect of drilling area temperature on drilling of carbon fiber reinforced polymer composites due to temperature-dependent properties. *Int. J. Adv. Manuf. Technol.* **2018**, *96*, 2943–2951. [CrossRef]
152. An, Q.; Dang, J.; Li, J.; Wang, C.; Chen, M. Investigation on the cutting responses of CFRP/Ti stacks: With special emphasis on the effects of drilling sequences. *Compos. Struct.* **2020**, *253*, 112794. [CrossRef]
153. Xu, J.; Li, C.; Chen, M.; El Mansori, M.; Davim, J.P. On the analysis of temperatures, surface morphologies and tool wear in drilling CFRP/Ti6Al4V stacks under different cutting sequence strategies. *Compos. Struct.* **2020**, *234*, 111708. [CrossRef]
154. Angelone, R.; Caggiano, A.; Improta, I.; Nele, L.; Teti, R. Characterization of hole quality and temperature in drilling of Al/CFRP stacks under different process condition. *Procedia CIRP* **2019**, *79*, 319–324. [CrossRef]
155. Giasin, K.; Ayvar-Soberanis, S. Evaluation of workpiece temperature during drilling of GLARE fiber metal laminates using infrared techniques: Effect of cutting parameters, fiber orientation and spray mist application. *Materials* **2016**, *9*, 622. [CrossRef] [PubMed]

156. Liu, J.; Zhang, D.; Qin, L.; Yan, L. Feasibility study of the rotary ultrasonic elliptical machining of carbon fiber reinforced plastics (CFRP). *Int. J. Mach. Tools Manuf.* **2012**, *53*, 141–150. [CrossRef]
157. Wang, X.; Kwon, P.Y.; Sturtevant, C.; Lantrip, J. Tool wear of coated drills in drilling CFRP. *J. Manuf. Process.* **2013**, *15*, 127–135. [CrossRef]
158. Fang, N.; Dewhurst, P. Slip-line modeling of built-up edge formation in machining. *Int. J. Mech. Sci.* **2005**, *47*, 1079–1098. [CrossRef]
159. List, G.; Nouari, M.; Gehin, D.; Gomez, S.; Manaud, P.; Le Petitcorps, Y.; Girot, F. Wear behaviour of cemented carbide tools in dry machining of aluminium alloy. *Wear* **2005**, *259*, 1177–1189. [CrossRef]
160. Nouari, M.; List, G.; Girot, F.; Gehin, G. Effect of machining parameters and coating on wear mechanisms in dry drilling of aluminium alloys. *Int. J. Mach. Tools. Manuf.* **2005**, *45*, 1436–1442. [CrossRef]
161. Jeong, M.-J.; Lee, S.-W.; Jang, W.-K.; Kim, H.-J.; Seo, Y.-H.; Kim, B.-H. Prediction of drill bit breakage using an infrared sensor. *Sensors* **2021**, *21*, 2808. [CrossRef]
162. Wika, K.; Sharman, A.; Goulbourne, D.; Ridgway, K. *Impact of Number of Flutes and Helix Angle on Tool Performance and Hole Quality in Drilling Composite/Titanium Stacks*; SAE Technical Paper 2011-01-2744; SAE International: Warrendale, PA, USA, 2011. [CrossRef]
163. Kalpakjian, S.; Schmid, S. *Manufacturing Processes for Engineering Materials*, 5th ed.; Pearson: London, UK, 2008.
164. Arola, D.D.; Ramulu, M.; Wang, D. Chip formation in orthogonal trimming of graphite/epoxy composite. *Compos. A Appl. Sci. Manuf.* **1998**, *27*, 121–133. [CrossRef]
165. Kim, D.; Ramulu, M.; Pedersen, W. Machinability of titanium/graphite hybrid composites in drilling. *Trans. NAMRI/SME* **2005**, *33*, 445–452.
166. El Bouami, S.; Habak, M.; Franz, G.; Velasco, R.; Vantomme, P. Effect of tool geometry and cutting parameters on delamination and thrust forces in drilling CFRP/Al-Li. *AIP Conf. Proc.* **2016**, *1769*, 080012.
167. Krishnaraj, V.; Zitoune, R.; Collombet, F. Study of drilling of multi-material (CFRP/Al) using Taguchi and statistical techniques. *Usak Univ. J. Mater. Sci.* **2012**, *2*, 95–109.
168. Bayraktar, S.; Turgut, Y. Determination of delamination in drilling of carbon fiber reinforced carbon matrix composites/Al 6013-T651 stacks. *Measurement* **2020**, *154*, 107493. [CrossRef]
169. Pawar, O.A.; Gaikhe, Y.S.; Tewari, A.; Sundaram, R.; Joshi, S.S. Analysis of hole quality in drilling GLARE fiber metal laminates. *Compos. Struct.* **2015**, *123*, 350–365. [CrossRef]
170. Ekici, E.; Motorcu, A.R.; Uzun, G. Multi-objective optimization of process parameters for drilling fiber-metal laminate using a hybrid GRAPCA approach. *FME Trans.* **2021**, *49*, 356–366. [CrossRef]
171. Bonhin, E.P.; David-Müzel, S.; Guidi, E.S.; Botelho, E.C.; Ribeiro, M.V. Influence of drilling parameters on thrust force and burr on fiber metal laminate Al 2024-T3/glass fiber reinforced epoxy. *Procedia CIRP* **2021**, *101*, 338–341. [CrossRef]
172. Aamir, M.; Giasin, K.; Tolouei-Rad, M.; Vafadar, A. A review: Drilling performance and hole quality of aluminium alloys for aerospace applications. *J. Mater. Res. Technol.* **2020**, *9*, 12484–12500. [CrossRef]
173. Geier, N.; Davim, J.P.; Szalay, T. Advanced cutting tools and technologies for drilling carbon fibre reinforced polymer (CFRP) composites: A review. *Compos. A Appl. Sci. Manuf.* **2019**, *125*, 105552. [CrossRef]
174. Bertollo, N.; Walsh, W.R. Drilling of bone: Practicality, limitations and complications associated with surgical drill-Bits. *Biomech. Appl.* **2011**, *4*, 53–83.
175. Zhang, L.; Wang, L.; Wang, X. Study on vibration drilling of fiber reinforced plastics with hybrid variation parameters method. *Compos. Part. A Appl. Sci. Manuf.* **2003**, *34*, 237–244.
176. Wang, X.; Wang, L.J.; Tao, J.P. Investigation on thrust in vibration drilling of fiber reinforced plastics. *J. Mater. Process. Technol.* **2004**, *148*, 239–244. [CrossRef]
177. Sadek, A.; Attia, M.H.; Meshreki, M.; Shi, B. Characterization and optimization of vibration-assisted drilling of fibre reinforced epoxy laminates. *CIRP Ann. Manuf. Technol.* **2013**, *62*, 91–94. [CrossRef]
178. Debnath, K.; Singh, I. Low-frequency modulation-assisted drilling of carbon-epoxy composite laminates. *J. Manuf. Process.* **2017**, *25*, 262–273. [CrossRef]
179. Makhdum, F.; Phadnis, V.A.; Roy, A.; Silberschmidt, V.V. Effect of ultrasonically-assisted drilling on carbon-fibre-reinforced plastics. *J. Sound Vib.* **2014**, *333*, 5939–5952. [CrossRef]
180. Laporte, S.; De Castelbajac, C. Major breakthrough in multi material drilling, using low frequency axial vibration assistance. *SAE Int. J. Mater. Manuf.* **2013**, *6*, 11–18. [CrossRef]
181. Pecat, O.; Brinksmeier, E. Low damage drilling of CFRP/titanium compound materials for fastening. *Procedia CIRP* **2014**, *13*, 1–7. [CrossRef]
182. Pecat, O.; Brinksmeier, E. Tool wear analyses in low frequency vibration assisted drilling of CFRP/Ti6Al4V stack material. *Procedia CIRP* **2014**, *14*, 142–147. [CrossRef]
183. Lonfier, J.; De Castelbajac, C. A comparison between regular and vibration-assisted drilling in CFRP/Ti6Al4V stack. *SAE Int. J. Mater. Manuf.* **2015**, *8*, 18–26. [CrossRef]
184. Hussein, R.; Sadek, A.; Elbestawi, M.A.; Attia, M.H. Surface and microstructure characterization of low-frequency vibration-assisted drilling of Ti6Al4V. *Int. J. Adv. Manuf. Technol.* **2019**, *103*, 1443–1457. [CrossRef]

185. Hussein, R.; Sadek, A.; Elbestawi, M.A.; Attia, M.H. An investigation into tool wear and hole quality during low-frequency vibration-assisted drilling of CFRP/Ti6Al4V stack. *J. Mater. Process. Technol.* **2019**, *3*, 3030063. [CrossRef]
186. Hussein, R.; Sadek, A.; Elbestawi, M.A.; Attia, M.H. Elimination of delamination and burr formation using high-frequency vibration-assisted drilling of hybrid CFRP/Ti6Al4V stacked material. *Int. J. Adv. Manuf. Technol.* **2019**, *105*, 859–873. [CrossRef]
187. Li, C.; Xu, J.; Chen, M.; An, Q.; El Mansori, M.; Ren, F. Tool wear processes in low frequency vibration assisted drilling of CFRP/Ti6Al4V stacks with forced air-cooling. *Wear* **2019**, *426–427*, 1616–1623. [CrossRef]
188. Shao, Z.; Jiang, X.; Geng, D.; Li, S.; Zhang, D. Feasibility study on ultrasonic-assisted drilling of CFRP/Ti stacks by single-shot under dry condition. *Int. J. Adv. Manuf. Technol.* **2019**, *105*, 1259–1273. [CrossRef]
189. Xu, J.; Li, C.; Chen, M.; Ren, F. A comparison between vibration assisted and conventional drilling of CFRP/Ti6Al4V stacks. *Mater. Manuf.* **2019**, *34*, 1182–1193. [CrossRef]
190. Yang, H.; Chen, Y.; Xu, J.; Ladonne, M.; Lonfier, J.; Fu, Y. Tool wear mechanism in low-frequency vibration–assisted drilling of CFRP/Ti stacks and its individual layer. *Int. J. Adv. Manuf. Technol.* **2019**, *104*, 2539–2551. [CrossRef]
191. Hussein, R.; Sadek, A.; Elbestawi, M.A.; Attia, M.H. The effect of MQL on tool wear progression in low-frequency vibration-assisted drilling of CFRP/Ti6Al4V stack material. *J. Manuf. Mater. Process.* **2021**, *5*, 50. [CrossRef]
192. Shao, Z.; Jiang, X.; Geng, D.; Liu, Y.; Zhou, Z.; Li, S.; Zhang, D.; Zheng, W. The interface temperature and its influence on surface integrity in ultrasonic-assisted drilling of CFRP/Ti stacks. *Compos. Struct.* **2021**, *266*, 113803. [CrossRef]
193. Voss, R.; Henerichs, M.; Rupp, S.; Kuster, F.; Wegener, K. Evaluation of bore exit quality for fibre reinforced plastics including delamination and uncut fibres. *CIRP J. Manuf. Sci. Technol.* **2016**, *12*, 56–66. [CrossRef]
194. Wang, G.D.; Suntoo, D.; Li, N.; Peng, T.; Li, Y. Experimental research in CFRP/Ti stack through different helical milling strategies. *Int. J. Adv. Manuf. Technol.* **2018**, *98*, 3251–3267. [CrossRef]
195. Denkena, B.; Boehnke, D.; Dege, J.H. Helical milling of CFRP–titanium layer compounds. *CIRP J. Manuf. Sci. Technol.* **2008**, *1*, 64–69. [CrossRef]
196. Sadek, A.; Meshreki, M.; Attia, M.H. Characterization and optimization of orbital drilling of woven carbon fiber reinforced epoxy laminates. *CIRP Ann. Manuf. Technol.* **2012**, *61*, 123–126. [CrossRef]
197. Qin, X.; Wang, B.; Wang, G.; Li, H.; Jiang, Y.; Zhang, X. Delamination analysis of the helical milling of carbon fiber-reinforced plastics by using the artificial neural network model. *J. Mech. Sci. Technol.* **2014**, *28*, 713–719. [CrossRef]
198. Voss, R.; Henerichs, M.; Kuster, F. Comparison of conventional drilling and orbital drilling in machining carbon fibre reinforced plastics (CFRP). *CIRP Ann. Manuf. Technol.* **2016**, *65*, 137–140. [CrossRef]
199. Geier, N.; Szalay, T. Optimisation of process parameters for the orbital and conventional drilling of uni-directional carbon fibre-reinforced polymers (UD-CFRP). *Measurement* **2017**, *110*, 319–334. [CrossRef]
200. He, G.; Li, H.; Jiang, Y.; Qin, X.; Zhang, X.; Guan, Y. Helical milling of CFRP/Ti-6Al-4V stacks with varying machining parameters. *Trans. Tianjin Univ.* **2015**, *21*, 56–63. [CrossRef]
201. Wang, H.; Qin, X.; Li, H.; Tan, Y. A comparative study on helical milling of CFRP/Ti stacks and its individual layers. *Int. J. Adv. Manuf. Technol.* **2016**, *86*, 1973–1983. [CrossRef]
202. Zhou, L.; Ke, Y.; Dong, H.; Chen, Z.; Gao, K. Hole diameter variation and roundness in dry orbital of CFRP/Ti stacks drilling. *Int. J. Adv. Manuf. Technol.* **2016**, *87*, 811–824. [CrossRef]
203. Pan, Z.; Wang, L.; Fang, Q.; Sun, Z.; Qu, W. Study on tool deflection compensation method based on cutting force observer for orbital drilling of CFRP/Ti stacks. *J. Manuf. Mater. Process.* **2022**, *75*, 450–460. [CrossRef]
204. Giasin, K.; Ayvar-Soberanis, S.; Hodzic, A. Evaluation of cryogenic cooling and minimum quantity lubrication effects on machining GLARE laminates using design of experiments. *J. Clean. Prod.* **2016**, *135*, 533–548. [CrossRef]
205. Giasin, K.; Dad, A.; Brousseau, E.; Pimenov, D.; Mia, M.; Morkavuk, S.; Koklu, U. The effects of through tool cryogenic machining on the hole quality in GLARE fibre metal laminates. *J. Manuf. Process.* **2021**, *64*, 996–1012. [CrossRef]
206. Biermann, D.; Iovkov, I.; Blum, H.; Rademacher, A.; Taebi, K.; Suttmeier, F.T.; Klein, N. Thermal aspects in deep hole drilling of aluminium cast alloy using twist drills and MQL. *Procedia CIRP* **2012**, *3*, 245–250. [CrossRef]
207. Chatha, S.S.; Pal, A.; Singh, T. Performance evaluation of aluminium 6063 drilling under the influence of nanofluid minimum quantity lubrication. *J. Clean. Prod.* **2016**, *137*, 537–545. [CrossRef]
208. Zhu, Z.; He, B.; Chen, J. Evaluation of tool temperature distribution in MQL drilling of aluminum 2024-T351. *J. Manuf. Process* **2020**, *56*, 757–765. [CrossRef]
209. Nagaraj, A.; Uysal, A.; Jawahir, I.S. An Investigation of process performance when drilling carbon fiber reinforced polymer (CFRP) composite under dry, cryogenic and MQL environments. *Procedia Manuf.* **2020**, *43*, 551–558. [CrossRef]
210. Fernández-Pérez, J.; Cantero, J.L.; Díaz-Álvarez, J.; Miguélez, M.H. Hybrid composite-metal stack drilling with different minimum quantity lubrication levels. *Materials* **2019**, *12*, 448. [CrossRef]
211. Min, J.; Xu, J.; Ming, C.; El Mansori, M. Effects of different cooling methods on the specific energy consumption when drilling CFRP/Ti6Al4V stacks. *Procedia Manuf.* **2020**, *43*, 95–102.
212. Xia, T.; Kaynak, Y.; Arvin, C.; Jawahir, I.S. Cryogenic cooling induced process performance and surface integrity in drilling CFRP composite material. *Int. J. Adv. Manuf. Technol.* **2016**, *82*, 605–616. [CrossRef]
213. Kumaran, S.T.; Ko, T.J.; Li, C.; Yu, Z.; Uthayakumar, M. Rotary ultrasonic machining of woven CFRP composite in a cryogenic environment. *J. Alloys Compd.* **2017**, *698*, 984–993. [CrossRef]

214. Joshi, S.; Rawat, K.; Balan, A.S.S. A novel approach to predict the delamination factor for dry and cryogenic drilling of CFRP. *J. Mater. Process. Technol.* **2018**, *262*, 521–531. [CrossRef]
215. Morkavuk, S.; Köklü, U.; Bağcı, M.; Gemic, L. Cryogenic machining of carbon fiber reinforced plastic (CFRP) composites and the effects of cryogenic treatment on tensile properties: A comparative study. *Compos. Part B-Eng.* **2018**, *147*, 1–11. [CrossRef]
216. Xu, J.; Ji, M.; Chen, M.; El Mansori, M. Experimental investigation on drilling machinability and hole quality of CFRP/Ti6Al4V stacks under different cooling conditions. *Int. J. Adv. Manuf. Technol.* **2020**, *109*, 1527–1539. [CrossRef]
217. Rodríguez, A.; Calleja, A.; Lacalle, L.; Pereira, O.; Rodríguez, G. Drilling of CFRP-Ti6Al4V stacks using CO_2-cryogenic cooling. *J. Manuf. Process.* **2021**, *64*, 58–66. [CrossRef]